TECHNICAL NOTE

D-1326

MOTIONS OF A SHORT 10° BLUNTED CONE ENTERING A MARTIAN ATMOSPHERE AT ARBITRARY ANGLES OF ATTACK AND ARBITRARY PITCHING RATES

By Victor L. Peterson

Ames Research Center
Moffett Field, Calif.

NATIONAL AERONAUTICS AND SPACE ADMINISTRATION

WASHINGTON May 1962

NATIONAL AERONAUTICS AND SPACE ADMINISTRATION

TECHNICAL NOTE D-1326

MOTIONS OF A SHORT 10° BLUNTED CONE ENTERING A MARTIAN ATMOSPHERE AT ARBITRARY ANGLES OF ATTACK AND ARBITRARY PITCHING RATES

By Victor L. Peterson

SUMMARY

The dynamic behavior of two probe vehicles entering a Martian atmosphere in a passive manner with arbitrary initial angles of attack and pitching rates to 12° per second has been determined. Results for an entry velocity of 21,700 feet per second and an entry angle of -40° were obtained from machine calculated solutions of the six-degree-of-freedom rigid-body equations of motion using experimental aerodynamic characteristics for the vehicles. One of the vehicles had a flat base and was statically stable in two attitudes (nose forward and base forward). The other vehicle, derived from the first by adding a conical afterbody, was statically stable in only one attitude (nose forward). A 10-rpm vehicle spin rate, believed ample for the purpose of distributing solar and aerodynamic heating over the vehicle surface, and model atmospheres encompassing the probable extremes for the planet were also considered.

It was found that while the motion of the flat-based vehicle could be oscillatory about either the nose-forward or base-forward stable trim attitudes when aerodynamic heating rates were high, the range of initial angles of attack resulting in base-forward orientation was reduced by more than a factor of 3 when initial pitch rates were increased from 0° to 12° per second. Results for the vehicle with afterbody having only nose-forward stability showed that oscillatory angles of attack at maximum heating-rate conditions probably would not exceed about 25° although angles of attack when heating rates were 50 percent of maximum could be as high as 40°. Values of these upper bound angles of attack were essentially independent of initial pitch rates for the range considered. Furthermore, the envelope of maximum probable angles of attack was increased only slightly when the vehicle was given a 10-rpm spin rate. The relationship between maximum amplitudes of oscillation and heating rates through high heating portions of the trajectories was preserved when model atmospheres believed to encompass the extreme possibilities for Mars were used in the calculations.

INTRODUCTION

A research program to define and investigate problems related to flight in planetary atmospheres has been initiated at the Ames Research Center. A problem of immediate concern is the design of probe vehicles which can enter atmospheres of planets other than Earth. Successful initial attempts of such entries cannot be assured, however, since characteristics of planetary atmospheres are not known precisely, even for the near-Earth planets, such as Mars and Venus. Thus, as suggested in reference 1, it seems reasonable to consider the possibility of designing the initial atmospheric probes to be part of more extensive projects; for example, split-mission experiments in which a mother vehicle ejects a probe vehicle in the vicinity of a planet and then continues in pursuit of other objectives.

The performance of such split-mission experiments might be enhanced if the probe could make a successful entry without requiring attitude control (other than that achieved passively by aerodynamic effects) either at the time of separation from the mother vehicle or upon entering the sensible atmosphere. Success of an entry performed under these conditions could, of course, depend upon the manner in which the probe was separated or ejected from the mother ship. One proven separation technique involves the use of explosive bolts. If the probe were ejected from the mother vehicle by this technique, a pitching velocity could be induced by an uneven separation. In this event, the vehicle would commence tumbling and continue to tumble at essentially an unchanging rate until it encountered the sensible atmosphere of the planet. Eventually the tumbling would be arrested by aerodynamic effects, provided the vehicle were stable about one or more trim attitudes, and the motion would become oscillatory about a stable trim angle of attack. Several factors which could influence the practicality of attempting this type of passive entry are readily apparent. One of these involves the amount of protection required by the vehicle against aerodynamic heating. In this regard, the range of possible attitudes in which the probe might be oriented when heating becomes significant would probably be larger for a passive entry than for an actively controlled entry. Thus, the feasibility of this passive entry concept depends upon the relationship between benefits derived from simplicity and complications arising from relinquishing active control over the vehicle.

The purpose of this report is to present the results of a study in which the passive entry concept was examined in some detail. The investigation entailed machine calculations of the motions and other pertinent trajectory parameters of two vehicles entering a Martian atmosphere at arbitrary angles of attack and arbitrary pitching rates ranging to 12° per second. The distinction between the two vehicles was that one had a flat base and the other had a conical afterbody. Static and dynamic aerodynamic characteristics obtained experimentally for models of both vehicles for angles of attack ranging to 180° at Mach numbers between 0.6 and 15.0 were used in the numerical calculations. These data primarily from

references 2, 3, and 4 are summarized herein. The two configurations, one with and one without an afterbody, were chosen to demonstrate the differences in dynamic behavior between a vehicle having two statically stable trim attitudes (nose forward and base forward) and a vehicle having one statically stable trim attitude (nose forward).

NOTATION

A — cross-sectional area at maximum diameter of vehicle and reference area for coefficient evaluation

A_{cc} — total acceleration of vehicle mass center with respect to inertial axes with origin at planet center

$C_A(\eta)$ — coefficient of aerodynamic force along the vehicle axis of revolution, $\frac{\text{force}}{q_\infty A}$

C_m — coefficient of pitching moment, $\frac{\text{moment about y axis}}{q_\infty Ad}$

$C_m(\eta)$ — coefficient of aerodynamic moment about an axis normal to plane of total angle of attack, $\frac{\text{moment}}{q_\infty Ad}$; equal to pitching-moment coefficient when sideslip angle is zero and yawing-moment coefficient when angle of attack is zero

C_{m_q} — rate of change of pitching-moment coefficient with pitching velocity parameter $\frac{qd}{V_A}$, $\frac{\partial C_m}{\partial(qd/V_A)}$

$C_{m_{\dot{\alpha}}}$ — rate of change of pitching-moment coefficient with time rate of change of angle-of-attack parameter $\frac{\dot{\alpha}d}{V_A}$, $\frac{\partial C_m}{\partial(\dot{\alpha}d/V_A)}$

$C_N(\eta)$ — coefficient of aerodynamic force normal to vehicle axis of revolution in plane of total angle of attack, η, $\frac{\text{force}}{q_\infty A}$; equal to normal-force coefficient when sideslip angle is zero and side-force coefficient when angle of attack is zero

C_n — coefficient of yawing moment, $\frac{\text{moment about z axis}}{q_\infty Ad}$

C_{n_r} rate of change of yawing-moment coefficient with yawing velocity parameter $\frac{rd}{V_A}$, $\frac{\partial C_n}{\partial(rd/V_A)}$

$C_{n_{\dot{\beta}}}$ rate of change of yawing-moment coefficient with time rate change of angle-of-sideslip parameter, $\frac{\dot{\beta}d}{V_A}$, $\frac{\partial C_n}{\partial(\dot{\beta}d/V_A)}$

d maximum diameter of vehicle and reference length for moment coefficient evaluation

g_o acceleration of gravity at surface of planet

H geopotential altitude, $\frac{h}{1 + (h/R_p)}$

h geometric altitude

I_X, I_Y, I_Z vehicle mass moments of inertia about the roll, pitch, and yaw axes, respectively

I_{YZ}, I_{XZ}, I_{XY} vehicle mass products of inertia about the roll, pitch, and yaw axes, respectively

M_∞ flight Mach number relative to atmosphere

m mass of vehicle

p, q, r components (along the roll, pitch, and yaw axes, respectively) of the angular velocity of the body with respect to inertial axes

q_∞ dynamic pressure

$\dot{q}_s$ stagnation-point laminar convective heating rate

R gas constant for atmosphere

R_B nose radius of vehicle at stagnation point

R_p radius of planet

T_∞ atmospheric temperature

u, v, w components (along x, y, z axes, respectively) of vehicle speed relative to atmosphere

V_A speed of vehicle relative to atmosphere

V_I	speed of vehicle relative to inertial axes
x, y, z	body-fixed orthogonal axes, origin at center of mass
α	angle of attack (see fig. 11 and appendix)
α_{env}	amplitude of angle-of-attack envelope
β	angle of sideslip (see fig. 11 and appendix)
γ	flight-path angle referenced to local horizontal, positive measured above horizontal
η	total angle of attack (see fig. 11 and appendix)
η_{env}	amplitude of total angle-of-attack envelope
ρ_∞	atmospheric mass density
ρ_o	fictitious sea-level atmospheric mass density consistent with isothermal portion of atmosphere above 54,000 feet (see fig. 1)

Subscripts

i	initial value of quantity
max	maximum value of quantity

DETAILS OF CALCULATIONS

A study of the general motions of a vehicle entering an atmosphere requires the solution of equations for a six-degree-of-freedom system. The equations used in this investigation, governing rigid bodies of revolution entering atmospheres of rotating planets, are presented in the appendix. Also included in the appendix is the equation used to calculate laminar convective stagnation-point heat-transfer rates throughout the trajectories. These equations were solved by numerical techniques on an IBM 7090 electronic data processing machine. The solutions obtained are dependent on the specific input quantities and initial conditions used. The inputs, which include planetary and vehicle characteristics, and the initial conditions are presented in this section of the report.

Planetary Characteristics

Mechanical properties.- From a survey of some of the literature, it has been found that values quoted for the mechanical properties of Mars, such as physical dimensions, surface gravity, and spin rate, differ by as much as 10 percent. It is believed that uncertainties in these parameters of this order would have essentially no effect on the results of this study. For this reason, no attempt was made to derive mean values for use herein. In this study the planet Mars was assumed to be a spherical body rotating about its polar axis in the same direction and with the same rate as the planet Earth. (The Martian spin rate has been measured and found equal to 1.026 that of Earth (ref. 5)). The planet diameter was taken to be 4215 U. S. statute miles (ref. 5) and the surface gravity[1] was assumed to be 13.16 ft/sec^2 (ref. 6).

Model atmosphere.- Various investigators have proposed models of the Martian atmosphere. Results of a study to determine the extremes of these models are presented in reference 7. Considerable uncertainty exists as to the atmospheric pressure, temperature, and density at altitude although all of the proposed models are composed predominantly of nitrogen which has thermodynamic properties similar to air. The model atmosphere used in this study is within the extremes presented in reference 7 and is identified specifically in figure 1.

At high altitudes the atmospheric density may differ by as much as several orders of magnitude, depending upon the particular model atmosphere chosen within the extremes presented in reference 7. Since the atmospheric density assumes an important role in the calculations by virtue of its appearance in the expression for dynamic pressure, several sample entries were calculated using model atmospheres representing the extreme values of density at the higher altitudes. The results of these calculations will be mentioned later.

Vehicle Characteristics

Geometry, mass, and inertia.- Two vehicles were used in the investigation. One was a short 10° half-angle blunted conical body of revolution with a flat base. The other had an identical forebody with a 50° half-angle conical afterbody. Dimensional sketches of the two vehicles are presented in figure 2. For purposes of comparison, the same values for mass, center of mass, and moments of inertia were used for both vehicles. These values are given in figure 2. The particular vehicle dimensions and mass properties selected for this investigation are considered representative of those for an instrumented atmospheric probe.

[1]Results of calculations have shown the relationship between vehicle attitude and altitude to be essentially the same with gravity either included or excluded over the altitude range of primary interest.

Aerodynamics.- Experimental values of the aerodynamic coefficients were used in the calculations. Static force and moment coefficients were obtained from tests of models of both vehicles at Mach numbers of 0.6, 1.0, 1.3, 3.1, and 5.5 in air and 15.0 in helium at angles of attack ranging from 0° to 180°. The data for air, published previously in reference 2, and unpublished data obtained in a helium wind tunnel are summarized herein in figure 3. Note that the moment reference center for the experimental data (0.48 d) differs from the vehicle center of mass used in the calculations (0.417 d). This difference has been accounted for in the calculations. The dynamic characteristics, consisting of the damping in pitch derivative $C_{m_q} + C_{m_{\dot{\alpha}}}$ (taken equal to the damping in yaw derivative for this investigation) were obtained for both vehicles from tests of models at Mach numbers ranging from 0.65 to 8.5 and angles of attack ranging to about 20°. These data, published previously in references 3 and 4, are summarized herein in figure 4. The method of accounting for the damping derivatives in the calculations requires some explanation. It will be noted that in the equations given in the appendix, it is indicated that the damping derivatives are simply C_{m_q} and C_{n_r}. This is because a satisfactory method of including the time-rate terms $C_{m_{\dot{\alpha}}}$ and $C_{n_{\dot{\beta}}}$ for simultaneously large values of both α and β was not available. On the other hand, the experimental techniques for measuring damping derivatives are such that the combination $C_{m_q} + C_{m_{\dot{\alpha}}}$ (or $C_{n_r} - C_{n_{\dot{\beta}}} \cos \alpha$) is obtained, and the separate contributions cannot be determined. Since it is known from the solutions of linear analyses that the total damping contribution always appears as a sum of the latter type, it was decided simply to use the experimental determination of $C_{m_q} + C_{m_{\dot{\alpha}}}$ where the equation calls for C_{m_q}. Likewise, by virtue of the vehicle's symmetry, the experimental determination of $C_{m_q} + C_{m_{\dot{\alpha}}}$ was used where the equation calls for C_{n_r}.[2] This method of handling the damping derivatives further implies that damping in the angle-of-attack plane is independent of damping in the sideslip plane.

The static coefficients used in the calculations (fig. 3) were tabulated in 5° increments of angle, and the computer program was written to use an interpolation scheme for selecting values at intermediate angles and Mach numbers. The dynamic derivatives C_{m_q} and C_{n_r} were taken to be zero for Mach numbers of 8.5 and above at all angles of attack. For Mach numbers less than 8.5 the curves for $C_{m_q} + C_{m_{\dot{\alpha}}}$ (fig. 4) were faired from the last measured value to zero at or before an angle of attack of 20°.

---

[2]The equations as written in the appendix and the method adopted here of using the experimental results become consistent under conditions where C_{m_q} is much larger than $C_{m_{\dot{\alpha}}}$. This should be the case for flight at very high speeds since time lags in the flow become very small. Since the significant part of the motions considered here occurs at high speeds, it is believed that the method adopted should introduce no sizable errors.

These values were tabulated for use in 1° increments up to $\alpha = 20^\circ$ (and $\beta = 20^\circ$) and were assumed to be zero for all higher angles of attack. A linear interpolation scheme was used to select values at intermediate Mach numbers and angles.

All of the above-mentioned data, actually representing vehicle characteristics in air, are presumed to apply in this study because of the similarity between air and the Martian atmosphere which is predominantly nitrogen. It may be noted that the data for $M_\infty = 15$ were obtained using a flow of helium gas. A limited amount of static data for an identical configuration tested in air at this Mach number shows the pitching-moment results obtained in helium and air are in good agreement to at least 30° angle of attack. Moreover, Newtonian theory modified for stagnation pressure loss through a normal shock predicts well the static characteristics of these configurations at $M_\infty = 5.5$ in air and $M_\infty = 15$ in helium. Thus, all of the results obtained at $M_\infty = 15$ in helium were taken to be those that would be obtained in air for the same and higher Mach numbers.

Initial Conditions

Parameters held constant.- The initial position of the vehicle relative to the planet and the initial orientation and magnitude of the velocity vector were the same for all calculations. These conditions were chosen to position the mass center of the vehicle in the equatorial plane 800,000 feet above the planet surface. Results of preliminary calculations showed that the aerodynamic forces and moments acting on the vehicle above this altitude are sufficiently small, for the model atmosphere used, so as not to alter the results of the investigation. An entry speed V_{I_i} of 21,700 feet per second relative to inertial axes originating at the planet center and an entry angle γ_i of -40° were used for the calculations. The velocity vector was oriented in the equatorial plane in the direction of the planet spin. The velocity vector thus defined is consistent with an Earth-Mars transit time of about 240 days and represents a speed of about 1.3 times the escape speed of Mars.

Parameters varied.- The study was restricted to one of planar motions for all but one trajectory. In the majority of the calculations, initial angles of attack ranged from -180° to $+180^\circ$ and initial pitch rates ranged from 0° to 12° per second. This range of pitching rates is more than adequate to include those obtained unintentionally by the explosive bolt technique for separating a capsule from a mother vehicle. Sideslip angle, roll angle, yawing rate, and spinning rate were all zero for the calculations involving planar motions. One entry was calculated for the vehicle with afterbody having a spin rate of 10 rpm.

RESULTS AND DISCUSSION

The purpose of the present investigation is to examine the dynamic behavior of two vehicles entering a Martian atmosphere, in a passive manner, with arbitrary initial angles of attack and arbitrary pitching rates to 12° per second. One of the vehicles has a flat base and is statically stable about both nose-forward and base-forward trim attitudes. The other vehicle, derived from the first by adding a conical afterbody, is statically stable about a nose-forward trim attitude only.

Results Common to Both Vehicles

Results of numerical calculations have shown, for purposes of this investigation, that certain trajectory parameters related to the motion of the vehicle mass center, such as Mach number, velocity, dynamic pressure, total acceleration, flight-path angle, and time, may be considered to be independent of motions of vehicles about their mass centers, provided extreme attitudes are not maintained at altitudes where aerodynamic effects are large. Furthermore, the parameters have nearly identical characteristics for both vehicles if the vehicles do not exceed moderate attitudes, because the vehicle forebodies are identical. Therefore, since cases of primary interest are those for which vehicle motion becomes oscillatory about the nose-forward trim attitude, a single presentation of these qualities applicable to both vehicles in this attitude is made. These results are presented in figure 5. Values of laminar convective stagnation-point heating rates for a nose radius of 1 foot are also shown on the figure.

The results of figure 5 indicate that the vehicles would be slowed by aerodynamic braking to sonic speeds at an altitude in excess of 54,000 feet. Since parachute deployment would be possible at or above this altitude, none of the trajectories calculated for this study are extended below 54,000 feet. Peak decelerations are well within tolerable limits for instrumented probes, and stagnation point convective heating rates for a nose radius of 1 foot are not excessive. In regard to aerodynamic heating, results of calculations for the vehicle without afterbody, traversing the atmosphere in the backward attitude, have shown that the maximum heating rate is encountered at somewhat higher altitude and lower velocity. The maximum heating rate for these conditions and for a nose radius of 1 foot is only about 2/3 the value for the vehicle in the forward attitude.

No undue problems are indicated by the results of figure 5 for parameters related to motions of the vehicle mass centers. It therefore appears that the success or failure of a passive entry into the Martian atmosphere will depend upon the amplitude history of the oscillatory motion relative to aerodynamic heating.

Vehicle Without Afterbody

Motion of vehicle about its mass center.- This vehicle is statically stable about two trim angles of attack, at $\eta = 0^\circ$ and at $\eta = 180^\circ$ (see fig. 3(a)). Thus, for a passive entry involving arbitrary initial angles of attack and pitching rates, obviously the vehicle could be in either a nose-forward or base-forward attitude over a considerable portion of the trajectory. This is illustrated by the results of figure 6 wherein samples of altitude history of angle of attack are presented for several values of initial angle of attack and pitching rate. Also indicated in figure 6 are the altitudes at which maximum dynamic pressure and maximum stagnation-point convective heating rates are encountered.

Consider first the results of figure 6 for an initial pitching rate of zero. Prior to entering the sensible atmosphere the vehicle experiences no pitching motion and, in general, is not in an aerodynamically trimmed attitude. As the vehicle penetrates the atmosphere, aerodynamic effects come into play and the vehicle seeks the stable trim angle of attack associated with the initial angle of attack. For example, the vehicle seeks the nose-forward attitude when initial angle of attack is 120° and it seeks the base-forward attitude when the initial angle of attack is 160°. The aerodynamically induced pitching motion is not critically damped so it becomes oscillatory about this trim angle. This oscillatory motion continues throughout the remainder of the trajectory with amplitude either converging to or diverging from the trim attitude, depending upon circumstances discussed later.

The sequence of events is somewhat different for the initially pitching vehicle as shown by the results of figure 6 for an initial pitch rate of 12° per second. If the vehicle has sufficient angular momentum it may pass through one or both trim attitudes one or more times before aerodynamic moments are large enough to bring the pitching motion to a momentary rest. The vehicle then begins to oscillate about the stable trim angle associated with the angle of attack where pitching motion was first arrested. Note in figure 6 for the initial pitch rate of 12° per second that the curves for initial angles of attack of 120° and 160° seem to terminate when angle of attack reaches 180°. In these cases where the vehicle passes through the 180° trim attitude and tumbles once before oscillatory motion is established, angles greater than 180° were treated as being equal to $\alpha - 360^\circ$. This method of presentation was chosen since the geometric angle between the vehicle and the airstream is of more interest than the angle accumulated from time equal to zero.

It is apparent from the results of figure 6 that the envelope of the oscillatory portion of angle-of-attack history converges throughout the trajectory when the vehicle is in the nose-forward attitude but diverges for altitudes below maximum dynamic pressure when the vehicle is in the base-forward attitude. This performance would be expected upon consideration of factors influencing aerodynamic damping as predicted by linearized

analytical studies (e.g., ref. 8). On the basis of the results of reference 8, the vehicle in the base-forward attitude is known to have a deficiency in aerodynamic damping when dynamic pressure is decreasing by virtue of its negative lift-curve slope and the assumption that C_{m_q} is zero.[3] On the other hand, in the nose-forward attitude, the vehicle has some aerodynamic damping even when C_{m_q} is zero because of its positive lift-curve slope in that attitude. It is interesting to note for altitudes below that for maximum dynamic pressure, the oscillatory motion of the vehicle in the base-forward attitude diverges to the extent of causing the vehicle to tumble. The vehicle then orients in the nose-forward attitude and its ensuing oscillatory motion begins to converge about the statically and dynamically stable zero angle-of-attack trim attitude. This reorientation of vehicle attitude occurs after maximum convective heating rates have been encountered.[4]

A 6 0 8

Relationship between initial conditions and vehicle attitude at maximum heating.- Further comparisons of the results obtained with and without an initial pitch rate (fig. 6) show the attitude of the vehicle (nose forward or base forward) as it encounters maximum convective heating rates to be dependent on initial values of pitching rate and angle of attack. For instance, an initial angle of attack of 160° results in a

---

[3]No dynamic data were available for this vehicle in the base-forward attitude, but experimental results for very blunt, low-fineness-ratio bodies have indicated that values of $C_{m_q} + C_{m_{\dot{\alpha}}}$ are generally very small and, in fact, positive in many cases. Thus, using a value of zero in the present calculations probably results in the minimum divergence of the angle-of-attack envelope for this vehicle in the base-forward attitude.

[4]An interesting possibility for the design of a passive vehicle which could traverse the lower portion of an atmosphere rapidly and still withstand the aerodynamic heating at higher altitudes is suggested by this result. A relatively sharp small-angle conical forebody and a very blunt, nearly flat afterbody would comprise the configuration. The afterbody bluntness and the forebody sharpness would be adjusted so that the effects of static stability would exceed those of dynamic instability while the vehicle was flying with its base forward in a positive dynamic pressure gradient where heating is severe. Then, when the dynamic pressure gradient became negative after peak heating, the dynamic instability would overpower the static stability so that motion would diverge to the extent of causing the vehicle to tumble and reorient in the low-drag, statically and dynamically stable, nose-forward attitude. Of course, this vehicle would have to be originally oriented in the base-forward attitude, but the allowable tolerance in initial attitude would be quite large. In fact, the tolerance in initial attitude may be large enough so that for flight from one point on a planet to another, it might be possible to launch the vehicle in the low-drag, nose-forward attitude and let it settle back into the atmosphere in the base-forward attitude. After this the sequence of events would be as described above.

base-forward attitude for an initial pitching rate of zero and a nose-forward attitude for an initial pitching rate of 12° per second. It is of interest to examine this dependence further.

As noted previously, the trim angle about which the motion of the initially pitching vehicle becomes oscillatory is dependent upon the angle of attack at the instant when aerodynamic moments first bring the pitching motion to a momentary rest. If the angle of attack at this instant is within the range of angles for which the vehicle is stable in the base-forward attitude, it seeks the 180° trim angle, otherwise it seeks the 0° trim angle. Of course, if the vehicle has no initial pitch rate, there is no question which attitude it will favor for a given initial angle of attack. If, however, the initial angular momentum of the vehicle is not zero, the stable trim attitudes about which the vehicle will be oscillating as the high heating portion of the trajectory is traversed are not immediately evident. In fact, if the initial angle of attack is arbitrary, the probability of the vehicle being in either the base-forward or nose-forward attitude at the time of maximum heating is a function of the initial pitch raté, all other conditions being the same. This rather interesting result is illustrated in figure 7 wherein the envelopes of initial conditions giving rise to both nose-forward and base-forward attitudes at the time the vehicle is undergoing maximum heating rates are presented. Note that increasing the initial pitching rate from 0° to 12° per second reduces the chances of the vehicle being in the backward attitude from about 1 in 5 to 1 in 18.

A 6 C 8

To summarize, the results presented thus far have illustrated that the vehicle having two stable trim angles probably would not be suitable for a passive entry since heat protection would be required over its entire surface. Furthermore, even if the entire vehicle were heat protected, parachute deployment at sonic speeds would be complicated by the extreme attitudes encountered for those entries involving some sustained flight with the vehicle base forward. Finally, it was demonstrated that the chance of the initially pitching vehicle eventually stabilizing in the base-forward attitude is reduced by an increase in the initial pitch rate.

Vehicle With Afterbody

Motion of vehicle about its mass center.- The fact that this vehicle is stable about only one trim angle of attack ($\eta = 0°$) is sufficient to insure a nose-forward attitude once oscillatory motion is established. Furthermore, from the results already presented for the vehicle without afterbody, it is known that angle-of-attack envelopes converge throughout the trajectories. It is still necessary, however, to determine the maximum amplitudes of oscillation that can be expected to result from the ranges of initial conditions being considered.

Sample altitude histories of vehicle angle of attack are presented in figure 8 for several values of initial angle of attack and pitch rate. The results of figure 8 for zero initial pitch rate show the effect of initial angle of attack on the envelope of oscillatory motion. As initial angle of attack is increased toward 180°, the envelope of the oscillations increases to include larger and larger amplitudes. The presence of the unstable 180° trim attitude becomes quite prominent at angles near 180°, as evidenced by the results for an initial angle of 178°. The overturning moment for this case is initially quite small so that several hundred thousand feet in altitude are traversed before oscillatory motion is achieved. The limiting case of 180° initial angle is a theoretical situation in which the vehicle remains in the unstable but trimmed base-forward attitude throughout a large portion of the trajectory. In actual flight, perturbations of angle of attack due to atmospheric disturbances would prevent the vehicle from remaining in an unstable trimmed attitude for extended periods of time. This possibility is not rejected by the present calculations, however, since the atmosphere is considered to be free of disturbances. Therefore, for the purpose of this study, only results for initial angles of attack displaced 2° or more from those that trap the vehicle in the 180° attitude are considered to be realistic. With this criterion, the most unfavorable angle-of-attack envelope possible for an initial pitch rate of zero results from an initial angle of attack of 178°.

A 6 0 8

An indication of the effect of a low vehicle spin rate (10 rpm) on the angle-of-attack envelope is also shown in figure 8. The case chosen to illustrate this effect ($\eta_i = 178°$) is believed to be representative of the most unfavorable result this spin rate can have on the angle-of-attack envelope. For this case, the inertial effects of spin are working against the aerodynamic tendency for the vehicle to seek the nose-forward stable attitude, so that overturning and initiation of oscillatory motion is delayed to a lower altitude. This causes the angle-of-attack envelope to be increased slightly throughout the trajectory. It is apparent from this result that spin rates of magnitudes likely to be used to distribute solar and aerodynamic heating over the vehicle surface probably would not upset conclusions that would have been drawn on the basis of no spin rate.

The results of figure 8 for an initial pitch rate of 12° per second are examples of how the angle-of-attack history can be altered when an initial pitch rate is introduced. For this initial pitch rate the tumbling motion may or may not be arrested immediately, depending upon the initial angle of attack. The significant point illustrated by these results is that amplitudes of oscillation are not necessarily larger for cases where the vehicle tumbling motion is not stopped immediately than for cases where it is stopped immediately (e.g., compare envelopes for $\alpha_i = 120°$ and $\alpha_i = 0°$). In fact, it has been found that the largest amplitudes of oscillation possible for this or any other pitch rate are given by initial angles of attack which cause the first peak of oscillatory motion to be just tangent to 178° (or the angle chosen to represent a realistic treatment of the 180° unstable trim condition).

The fact that oscillatory motion will be established at quite high altitudes for the initial pitching rates considered has been demonstrated. The point to be examined now is whether or not oscillatory motion is established at altitudes sufficiently high that amplitudes of oscillation are not excessive through the high heating portion of the trajectories.

Relationship between vehicle attitude and stagnation-point convective heating.- The dependence of angle-of-attack envelope, at the altitude for maximum convective heating rate, on the initial conditions is summarized in figure 9. Consider first the curve for zero initial pitch rate. The angle of attack for maximum heating conditions is increased as the magnitude of initial angle of attack is increased from 0°. However, it does not exceed about 25° until the initial angle of attack exceeds 178°. Between initial values of angle of attack of 178° and 180° the angle of attack at maximum heating is shown to increase from 25° to 180°. On the basis of considerations previously discussed, it is believed that these extreme possibilities may be ruled out on practical grounds.

Now consider the curves for nonzero initial pitch rates. Note that for each pitching rate, some initial angle of attack exists for which the vehicle theoretically trims in the unstable attitude of 180°. For example, 20.5° is the critical angle for a pitch rate of 12° per second. For an initial angle of attack greater than this, the vehicle tumbles once before the motion becomes oscillatory. For an angle of attack less than this, the vehicle will not pass through the base-forward attitude, and hence, will not tumble before oscillatory motion is established. In this regard, it is somewhat surprising that angles of attack at maximum heating after the vehicle has tumbled once are not significantly different from those when the vehicle has not tumbled. The portions of the curves within $\pm 2^\circ$ of the critical initial angles of attack for each initial pitch rate should probably be disregarded in keeping with the criterion used to select the extreme realistic cases. It may then be stated that amplitudes of oscillation at maximum convective heating conditions will not exceed about 25° for any pitching rate considered.

Maximum angles of attack that can result throughout the portion of the trajectories where heating may be important are presented in figure 10. The two curves shown, one for no spin rate and one for a spin rate of 10 rpm, apply for any combination of initial conditions (angle of attack and pitch rate), giving rise to the upper bound angles of attack at maximum heating. The criterion used to select realistic cases for the nonspinning vehicle was also used for the case involving vehicle spin. In this study vehicle spin was not considered as a means for attitude control but rather as a means for distributing solar and/or aerodynamic heating uniformly over the vehicle surface. It is shown that for no spin rate amplitudes of oscillation of the order of 40° may be experienced by the vehicle when heating rates have increased to 50 percent of maximum. Also, amplitudes may remain as high as 20° after maximum heating until heating rates diminish nearly to zero. The envelope is increased several degrees by the 10-rpm spin rate. The effect of spin would be proportionately less

for lower spin rates. The vehicle would, of course, have an equal chance of being subjected to amplitude-heating histories lying anywhere within these envelopes for other combinations of initial conditions.

The effects of choice of model atmosphere on the relationship between vehicle attitude and heating rates were also examined. At high altitudes, values of atmospheric density used in the foregoing calculations may be different from the possible extremes presented in reference 7 by as much as several orders of magnitude. In view of the uncertainties regarding the Martian atmosphere and the importance of atmospheric density in the calculations of the motions of vehicles, several sample entries were calculated using model atmospheres representing the extreme values of density as presented in reference 7. The results of these calculations showed that the relationship between vehicle attitudes and laminar convective stagnation point heating rates, through portions of the trajectory where heating rates are significant, was preserved from one model atmosphere to another. Thus, the results of this investigation pertaining to relationships between vehicle attitudes and heating rates would not be altered significantly by the choice of a different model atmosphere within the extremes.

A 6 0 8

CONCLUSIONS

The dynamic behavior of the two probe vehicles entering a Martian atmosphere in a passive manner with arbitrary initial angles of attack and pitching rates to 12° per second has been calculated. Analysis of results of these calculations showed that:

1. The motion of a vehicle statically stable in two attitudes (nose forward and base forward) could be oscillatory about either attitude while aerodynamic heating rates are high depending upon the initial conditions. However, the range of initial angles of attack resulting in base-forward orientation was reduced by more than a factor of 3 when initial pitch rates were increased from 0° to 12° per second.

2. The motion of a vehicle statically stable in only one attitude (nose forward) always became oscillatory about this attitude before aerodynamic heating rates became significant. Oscillatory angles of attack at maximum heating-rate conditions did not exceed about 25°, for all practical purposes, and angles of attack when heating rates were 50 percent of maximum were 40° or less. These results were essentially independent of initial pitch rate.

3. Introduction of a 10-rpm vehicle spin rate, believed ample to distribute solar and aerodynamic heating over the vehicle surface, increased values of oscillatory angle of attack by only a few degrees.

4. The relationship between maximum amplitudes of oscillation and heating rates through high heating portions of the trajectories was preserved when model atmospheres believed to encompass the extreme possibilities for Mars were used in the calculations.

Ames Research Center
National Aeronautics and Space Administration
Moffett Field, Calif., Mar. 6, 1962

APPENDIX

EQUATIONS USED IN THE INVESTIGATION

Coordinate systems are shown in figure 11 and the symbols used only in the appendix are defined as follows:

a_X, a_Y, a_Z	components (along x, y, z axes, respectively) of acceleration of vehicle mass center with respect to inertial axes
C_{xX}, C_{xY}, . . ., C_{zZ}	cosine of the angle between the indicated body axis and the indicated inertial axis
F_X, F_Y, F_Z	components of aerodynamic force along the positive x, y, z axes, respectively
g_X, g_Y, g_Z	components of acceleration due to gravity along the X, Y, Z axes, respectively
l_{cg}	distance from vehicle nose to vehicle center of mass
$l_{cp}(\eta)$	distance from vehicle nose to effective point of action of static aerodynamic force, $l_{cg} - \frac{C_m(\eta)}{C_N(\eta)} d$
M_X, M_Y, M_Z	components of aerodynamic moments about the x, y, z axes, respectively
r_V	distance from center of planet to vehicle mass center
X, Y, Z	inertial Cartesian coordinate system with origin at planet's center (Z axis is along planet's axis of spin.)
ψ, θ, φ	Euler angles relating body axes and inertial axes (See fig. 11.)
Ω	planet spin rate
$(\dot{})$, $(\ddot{})$	$\frac{d()}{dt}$, $\frac{d^2()}{dt^2}$

EQUATIONS OF MOTION

The equations of motion are the six-degree-of-freedom equations governing rigid bodies of revolution. The planet atmosphere is considered to rotate rigidly with the planet.

Force Equations

$$\begin{bmatrix} \ddot{X} \\ \ddot{Y} \\ \ddot{Z} \end{bmatrix} = \frac{1}{m} \begin{bmatrix} C_{xX} & C_{yX} & C_{zX} \\ C_{xY} & C_{yY} & C_{zY} \\ C_{xZ} & C_{yZ} & C_{zZ} \end{bmatrix} \begin{bmatrix} F_x \\ F_y \\ F_z \end{bmatrix} + \begin{bmatrix} g_X \\ g_Y \\ g_Z \end{bmatrix}$$

Moment Equations

$$I_x\dot{p} - I_{xy}\dot{q} - I_{xz}\dot{r} = (I_y - I_z)qr + I_{xz}pq - I_{xy}pr + I_{yz}(q^2 - r^2) + M_x$$

$$I_{xy}\dot{p} - I_y\dot{q} + I_{yz}\dot{r} = (I_x - I_z)pr + I_{yz}pq - I_{xy}qr + I_{xz}(p^2 - r^2) - M_y$$

$$I_{xz}\dot{p} + I_{yz}\dot{q} - I_z\dot{r} = (I_y - I_x)pq - I_{yz}pr + I_{xz}qr + I_{xy}(q^2 - p^2) - M_z$$

A
6
0
8

SUPPLEMENTARY EQUATIONS

Direction Cosines

$$\begin{bmatrix} \dot{C}_{xX} & \dot{C}_{yX} & \dot{C}_{zX} \\ \dot{C}_{xY} & \dot{C}_{yY} & \dot{C}_{zY} \\ \dot{C}_{xZ} & \dot{C}_{yZ} & \dot{C}_{zZ} \end{bmatrix} = \begin{bmatrix} rC_{yX} - qC_{zX} & pC_{zX} - rC_{xX} & qC_{xX} - pC_{yX} \\ rC_{yY} - qC_{zY} & pC_{zY} - rC_{xY} & qC_{xY} - pC_{yY} \\ rC_{yZ} - qC_{zZ} & pC_{zZ} - rC_{xZ} & qC_{xZ} - pC_{yZ} \end{bmatrix}$$

where initial values of the direction cosines are obtained from the initial Euler angles according to the following:

$$\begin{bmatrix} C_{xX_i} & C_{yX_i} & C_{zX_i} \\ C_{xY_i} & C_{yY_i} & C_{zY_i} \\ C_{xZ_i} & C_{yZ_i} & C_{zZ_i} \end{bmatrix} =$$

$$\begin{bmatrix} \cos\theta_i \cos\psi_i & -\cos\varphi_i \sin\psi_i + \sin\varphi_i \sin\theta_i \cos\psi_i & \sin\varphi_i \sin\psi_i + \cos\varphi_i \sin\theta_i \cos\psi_i \\ \cos\theta_i \sin\psi_i & \cos\varphi_i \cos\psi_i + \sin\varphi_i \sin\theta_i \sin\psi_i & -\sin\varphi_i \cos\psi_i + \cos\varphi_i \sin\theta_i \sin\psi_i \\ -\sin\theta_i & \sin\varphi_i \cos\theta_i & \cos\varphi_i \cos\theta_i \end{bmatrix}$$

Aerodynamic Forces

$$F_x = -C_A(\eta) q_\infty A$$

$$F_y = -C_N(\eta) q_\infty A \frac{v}{\sqrt{v^2 + w^2}}$$

$$F_z = -C_N(\eta) q_\infty A \frac{w}{\sqrt{v^2 + w^2}}$$

Aerodynamic Moments

$$M_x = 0$$

$$M_y = F_z[l_{cp}(\eta) - l_{cg}] + C_{m_q} q_\infty A \frac{d^2 q}{V_A}$$

$$M_z = -F_y[l_{cp}(\eta) - l_{cg}] + C_{n_r} q_\infty A \frac{d^2 r}{V_A}$$

Angles

$$\alpha = \tan^{-1} \frac{w}{u}, \quad -\pi \leq \alpha \leq \pi$$

Quadrant of α is established according to the following table:

Sign of w	Sign of u	Quadrant of α
+	+	$0 < \alpha < \pi/2$
+	-	$\pi/2 < \alpha < \pi$
-	+	$-\pi/2 < \alpha < 0$
-	-	$-\pi < \alpha < -\pi/2$

$$\beta = \tan^{-1} \frac{v}{\sqrt{u^2 + w^2}} , \quad -\pi \leq \beta \leq \pi$$

Quadrant of β is established according to the following table:

Sign of v	Sign of u	Quadrant of β
+	+	$0 < \beta < \pi/2$
+	-	$\pi/2 < \beta < \pi$
-	+	$-\pi/2 < \beta < 0$
-	-	$-\pi < \beta < -\pi/2$

$$\eta = \pm\tan^{-1} \frac{\sqrt{v^2 + w^2}}{|u|} , \quad -\pi \leq \eta \leq \pi$$

Quadrant of η is established according to the following table:

Sign of u	Sign of w	Quadrant of η
+	+	$0 < \eta < \pi/2$
+	-	$-\pi/2 < \eta < 0$
-	+	$\pi/2 < \eta < \pi$
-	-	$-\pi < \eta < -\pi/2$

Gravitational Accelerations

$$g_X = -g_o R_p^2 \frac{X}{r_v^3}$$

$$g_Y = -g_o R_p^2 \frac{Y}{r_v^3}$$

$$g_Z = -g_o R_p^2 \frac{Z}{r_v^3}$$

Velocities

$$\begin{bmatrix} u \\ v \\ w \end{bmatrix} = \begin{bmatrix} C_{xX} & C_{xY} & C_{xZ} \\ C_{yX} & C_{yY} & C_{yZ} \\ C_{zX} & C_{zY} & C_{zZ} \end{bmatrix} \begin{bmatrix} \dot{X} + \Omega Y \\ \dot{Y} - \Omega X \\ \dot{Z} \end{bmatrix}$$

$$V_A = \sqrt{u^2 + v^2 + w^2}$$

$$V_I = \sqrt{\dot{X}^2 + \dot{Y}^2 + \dot{Z}^2}$$

Accelerations Relative To Inertial Axes

$$\begin{bmatrix} a_x \\ a_y \\ a_z \end{bmatrix} = \begin{bmatrix} C_{xX} & C_{xY} & C_{xZ} \\ C_{yX} & C_{yY} & C_{yZ} \\ C_{zX} & C_{zY} & C_{zZ} \end{bmatrix} \begin{bmatrix} \ddot{X} \\ \ddot{Y} \\ \ddot{Z} \end{bmatrix}$$

$$A_{cc} = \sqrt{a_x^2 + a_y^2 + a_z^2}$$

Stagnation Point Laminar Convective Heating Rate

An approximate formula given in reference 9 is used herein. This formula is

$$\sqrt{R_B}\ \dot{q}_s = C \sqrt{\rho_\infty}\ V_A^3 \ \text{Btu/ft}^{3/2}/\text{sec}$$

where

$$C = 1.97 \times 10^{-8}\ ,\ V_A \ \text{in ft/sec}\ ,\ \rho_\infty \ \text{in slugs/ft}^3$$

REFERENCES

1. Gates, C. R.: A Description of a Mars Spacecraft With a Landing Capsule. American Rocket Society Paper No. 61-180-1874, June 1961.

2. Treon, Stuart: Static Aerodynamic Characteristics of Short Blunt Cones With Various Nose and Base Cone Angles at Mach Numbers From 0.6 to 5.5 and Angles of Attack to 180°. NASA TN D-1327, 1962.

3. Wehrend, William R., Jr.: Wind-Tunnel Investigation of the Static and Dynamic Stability Characteristics of a 10° Semivertex Angle Blunted Cone. NASA TN D-1202, 1962.

4. Intrieri, Peter F.: Free-Flight Measurements of the Static and Dynamic Stability and Drag of a 10° Blunted Cone at M = 3.5 and 8.5. NASA TN D-1299, 1962.

5. Kiess, Carl C., and Lassovzsky, K.: The Known Physical Characteristics of the Moon and the Planets. ARDC TR 58-41, July, 1958.

6. Ehricke, Krafft A.: Space Flight. Vol. I of Environment and Celestial Mechanics. D. Von Nostrand, Princeton, 1960, pp. 120-122.

7. Anon.: JPL Space Program Summary 37-12, Vol. I, September 1 to November 1, 1961. December 1961.

8. Sommer, Simon C., and Tobak, Murray: Study of the Oscillatory Motion of Manned Vehicles Entering the Earth's Atmosphere. NASA MEMO 3-2-59A, 1959.

9. Chapman, Dean R.: An Approximate Analytical Method for Studying Entry Into Planetary Atmospheres. NASA Rep. R-11, 1958. (Supersedes NACA TN 4276.)

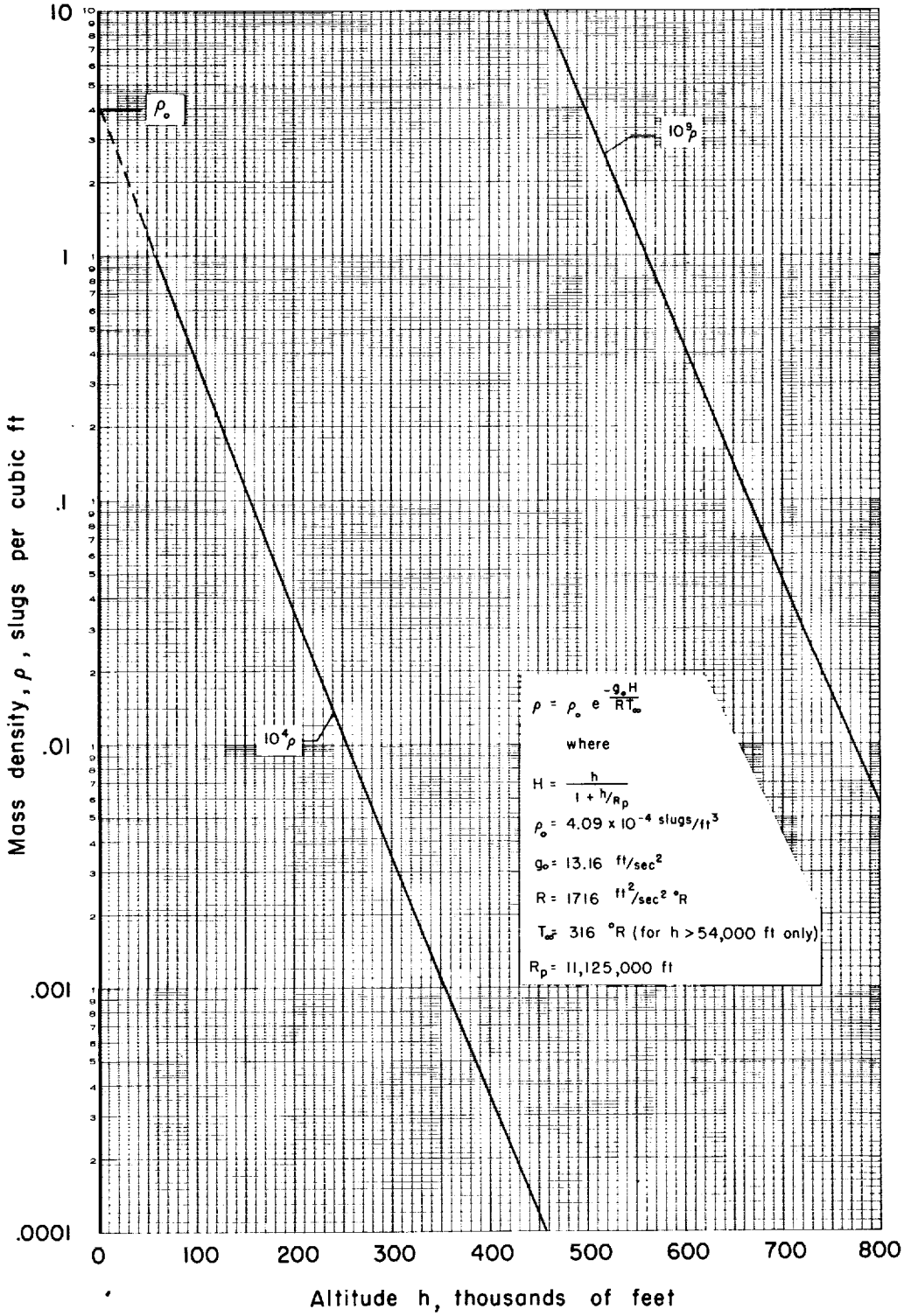

Figure 1.- Density-altitude relationship for model Martian atmosphere.

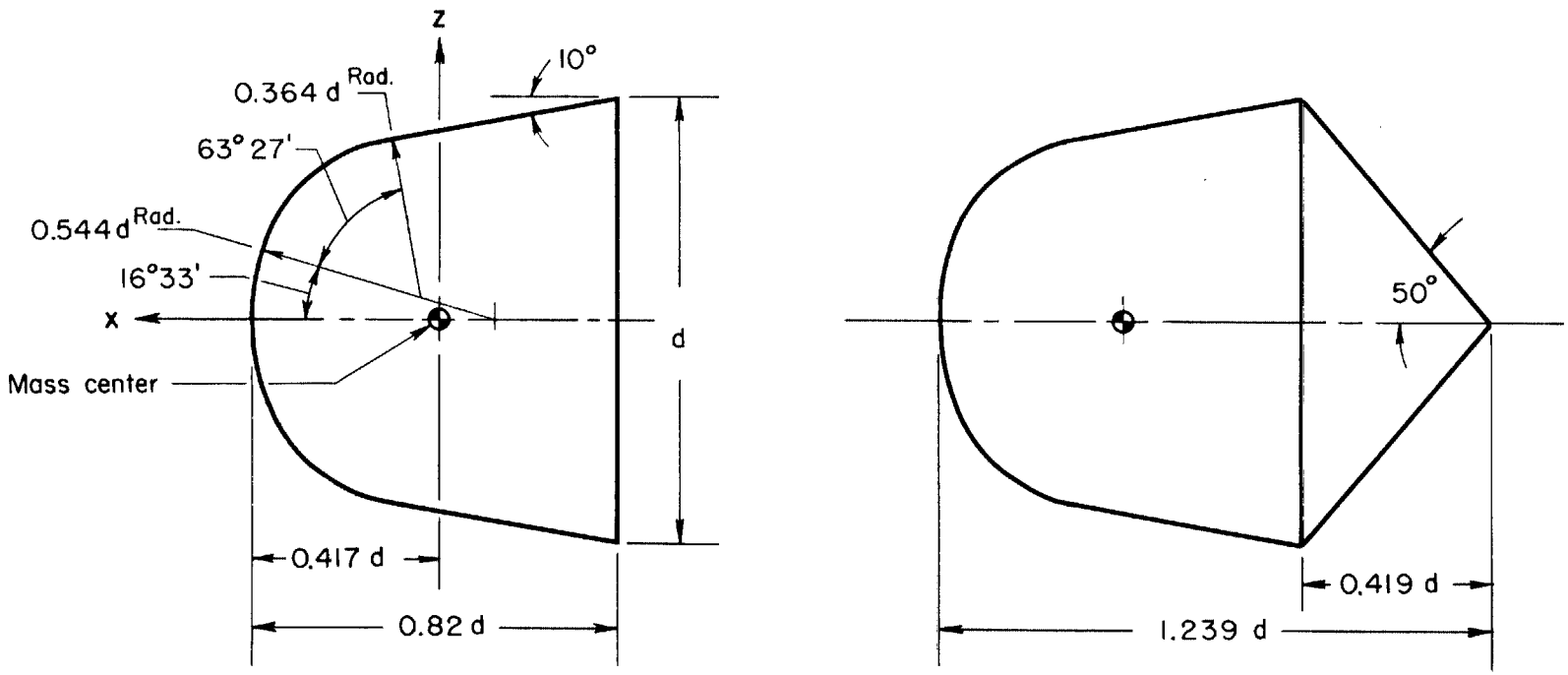

Vehicle without afterbody

Vehicle with afterbody

Diam., d = 3.25 ft
Mass = 6.685 slugs
I_x = 2.8 slug-ft^2
$I_y = I_z$ = 5.6 slug-ft^2
$I_{xy} = I_{xz} = I_{yz} = 0$

Figure 2.- Vehicle details.

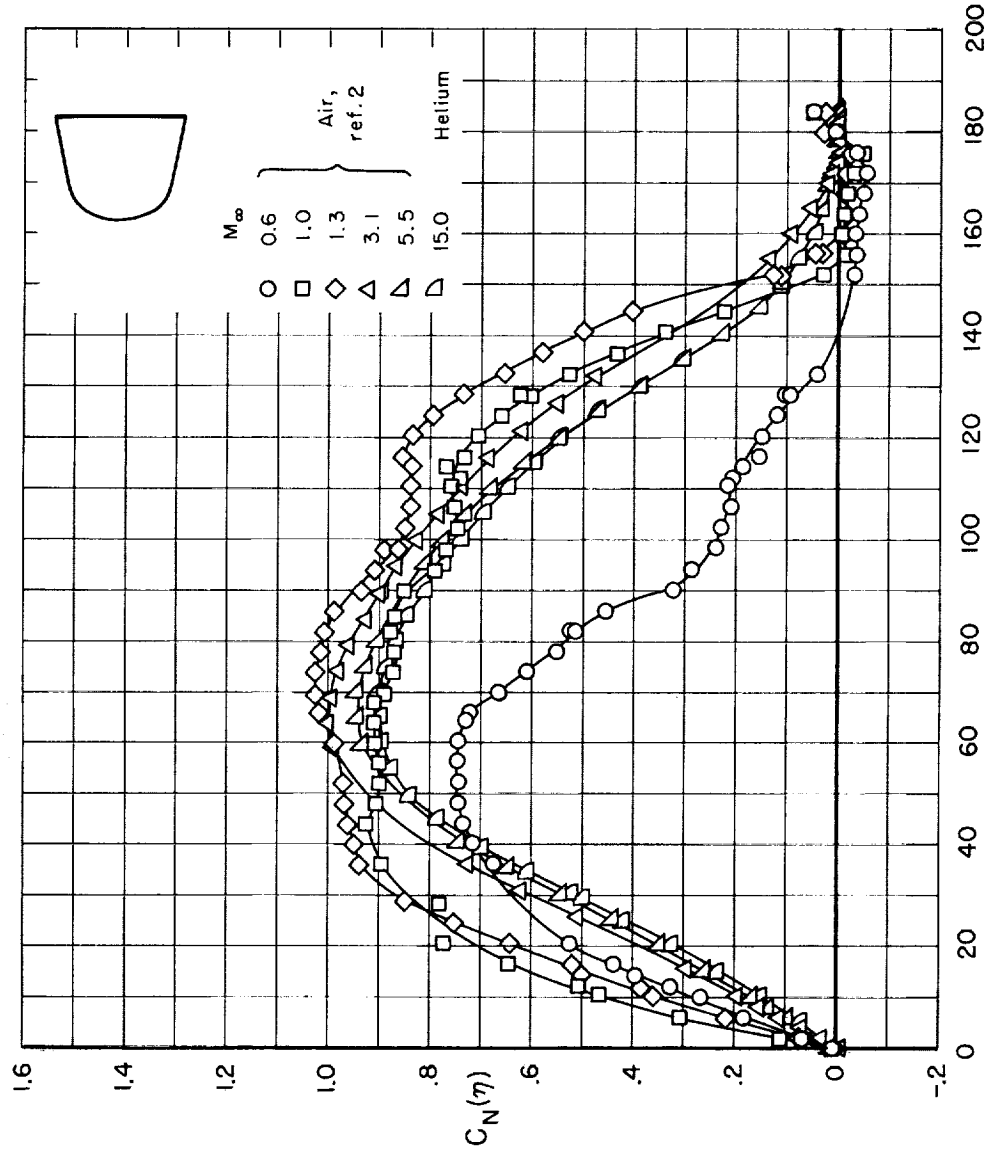

(a) Vehicle without afterbody.

Figure 3.- Static aerodynamic characteristics of the vehicles.

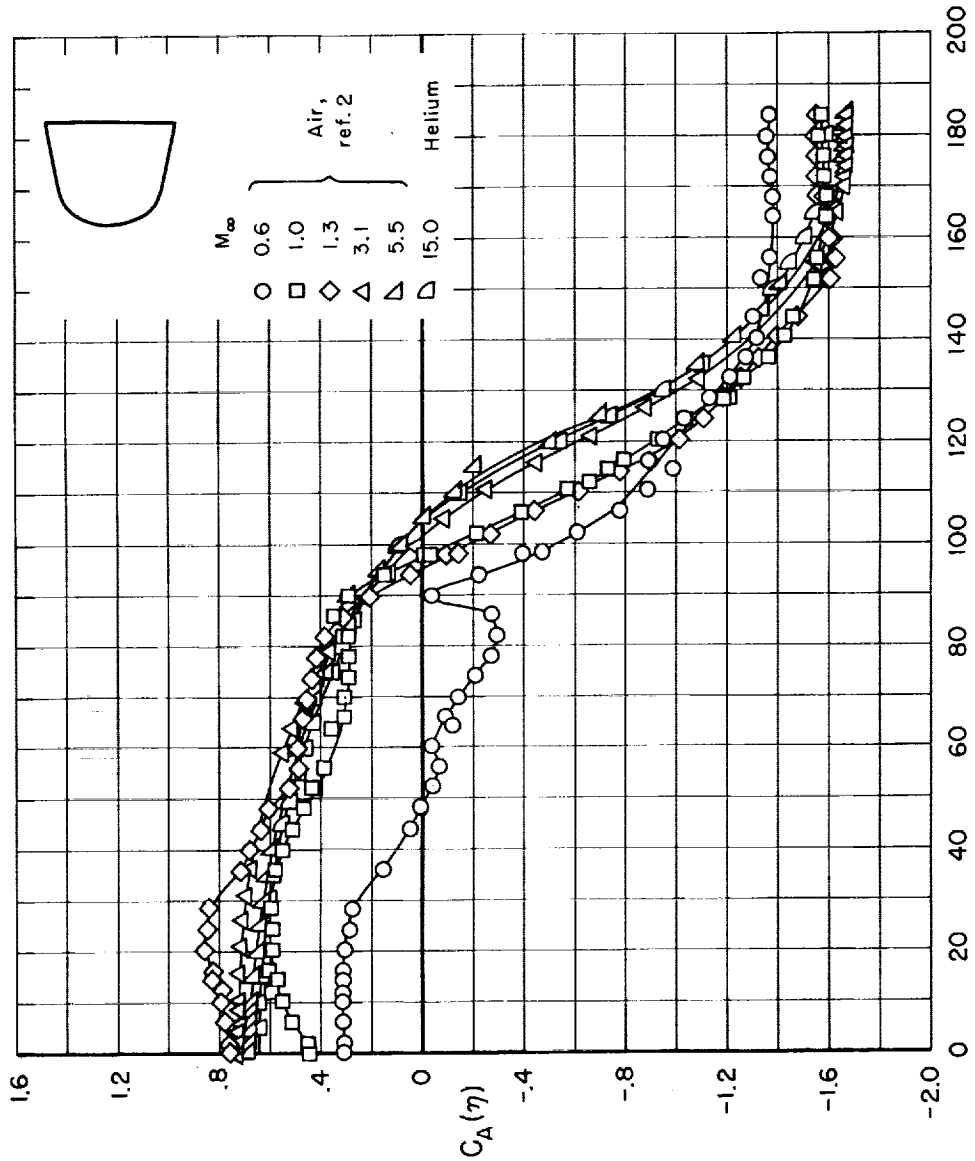

(a) Vehicle without afterbody - Continued.

Figure 3.- Continued.

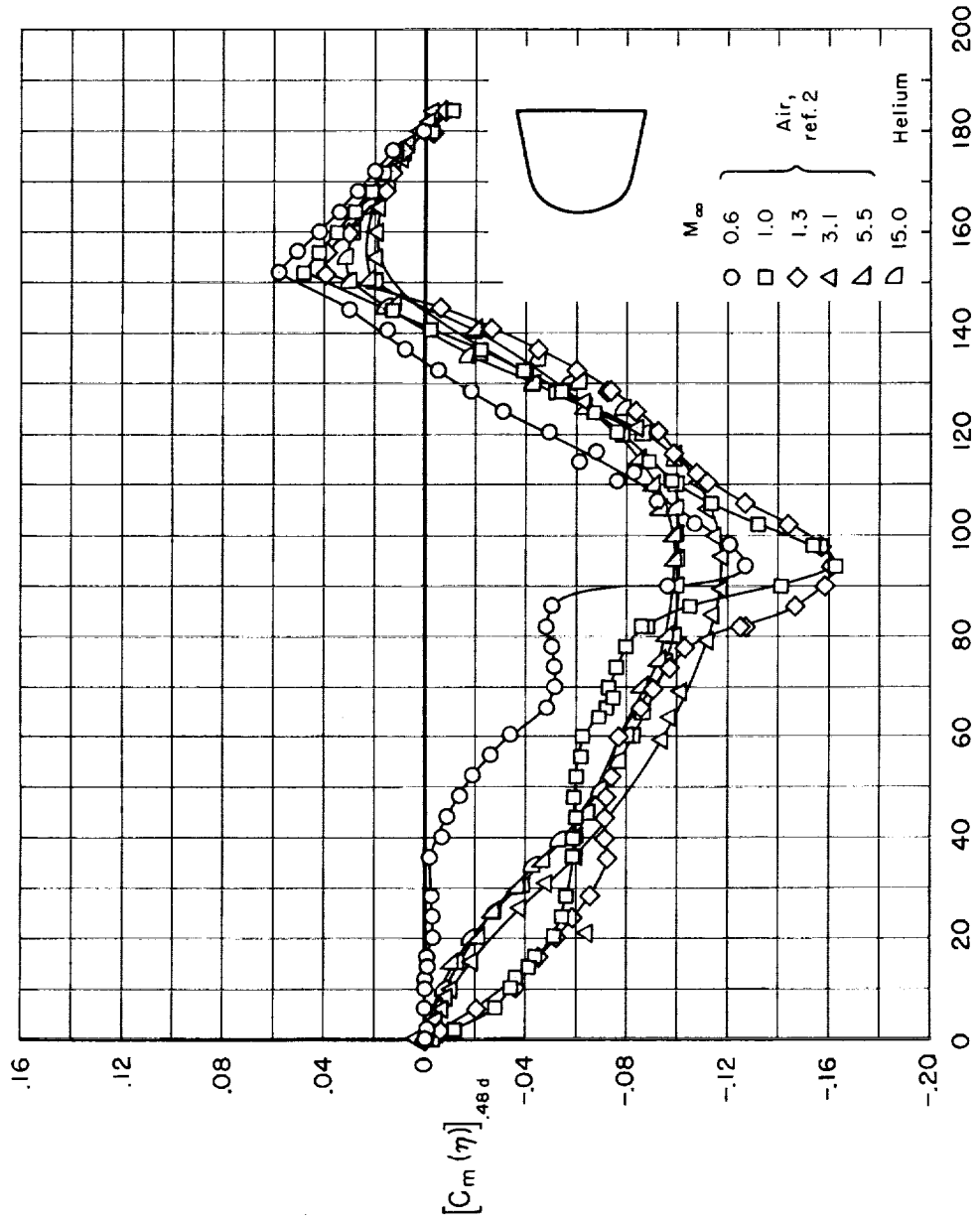

(a) Vehicle without afterbody - Concluded.

Figure 3.- Continued.

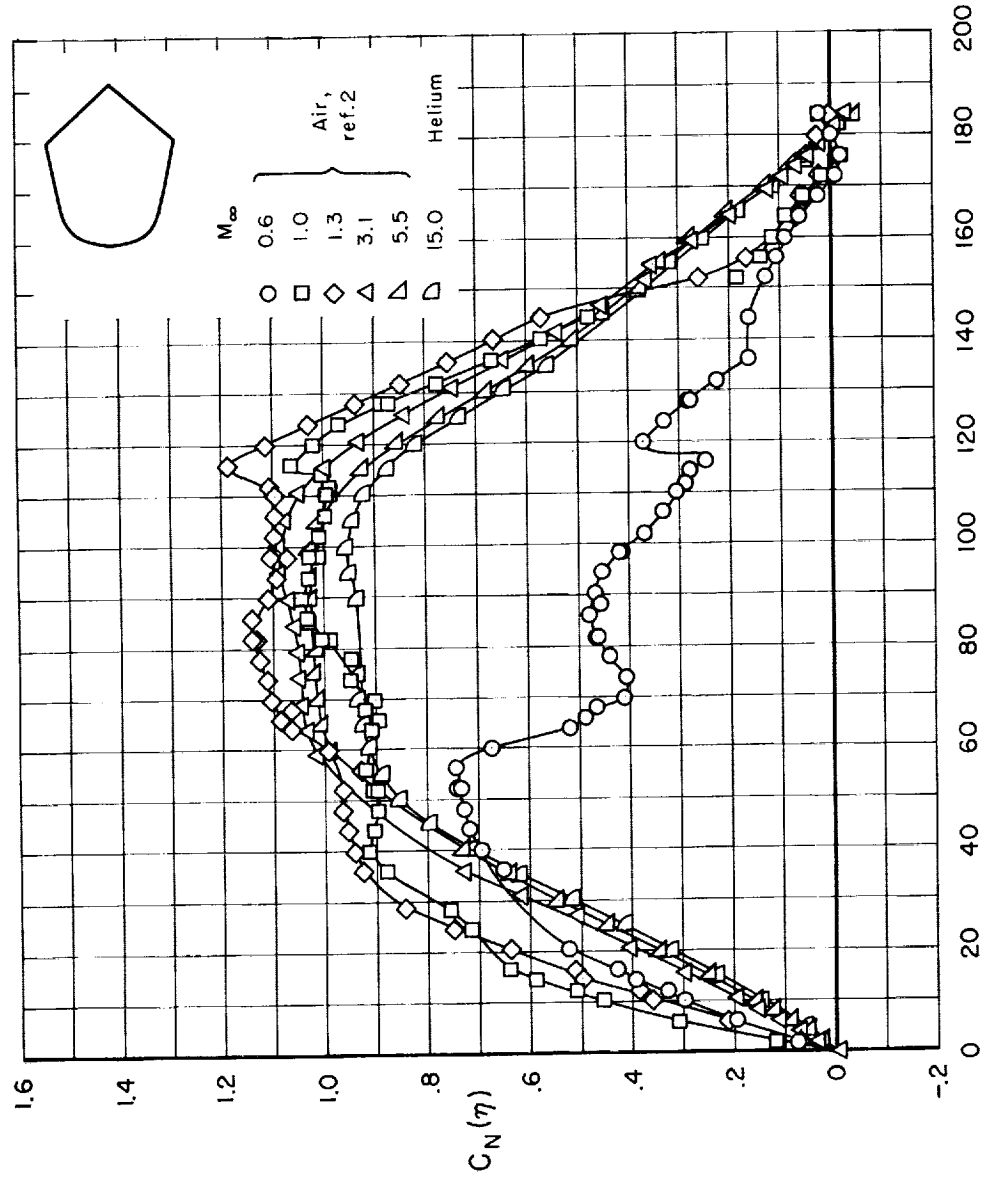

(b) Vehicle with afterbody.

Figure 3.- Continued.

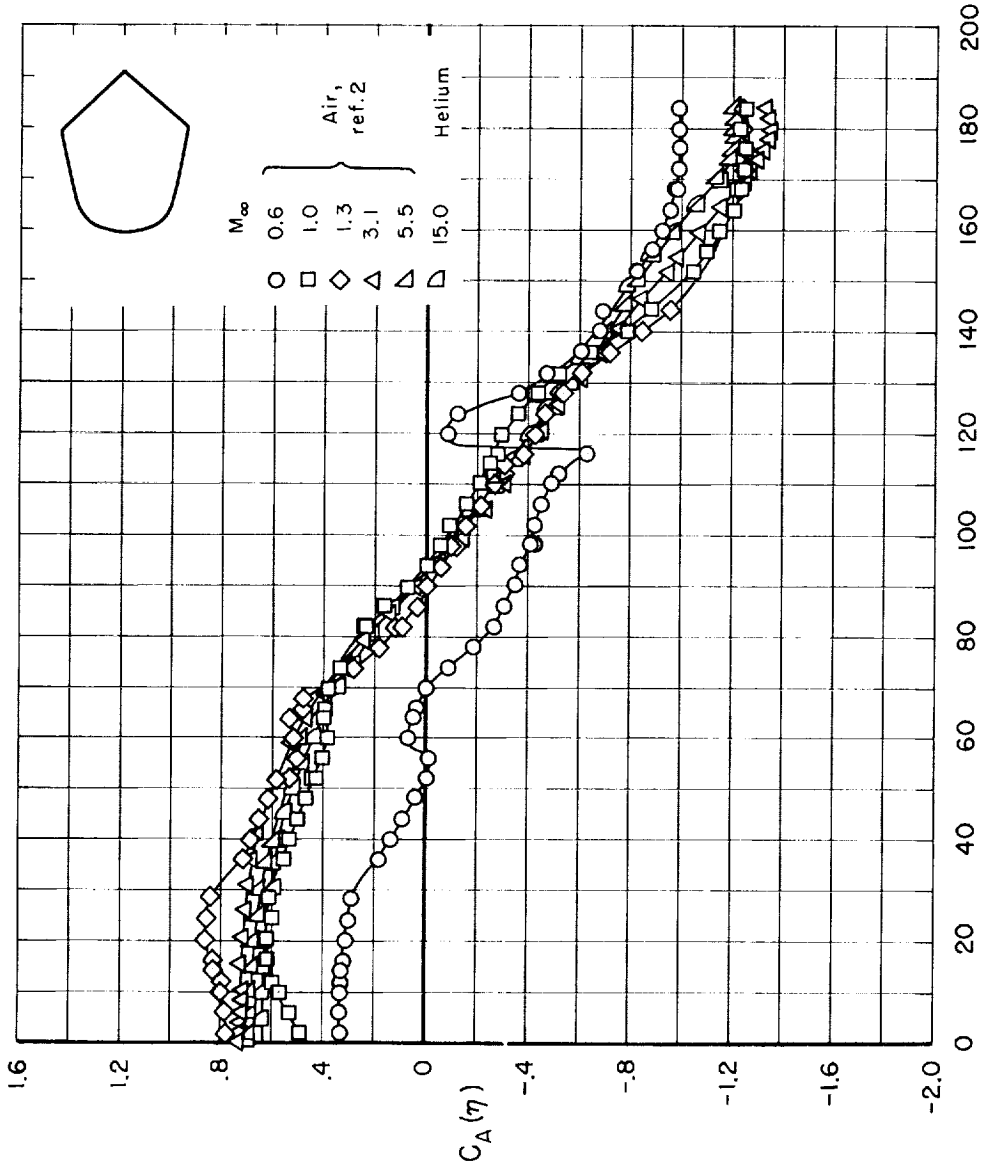

(b) Vehicle with afterbody - Continued.

Figure 3.- Continued.

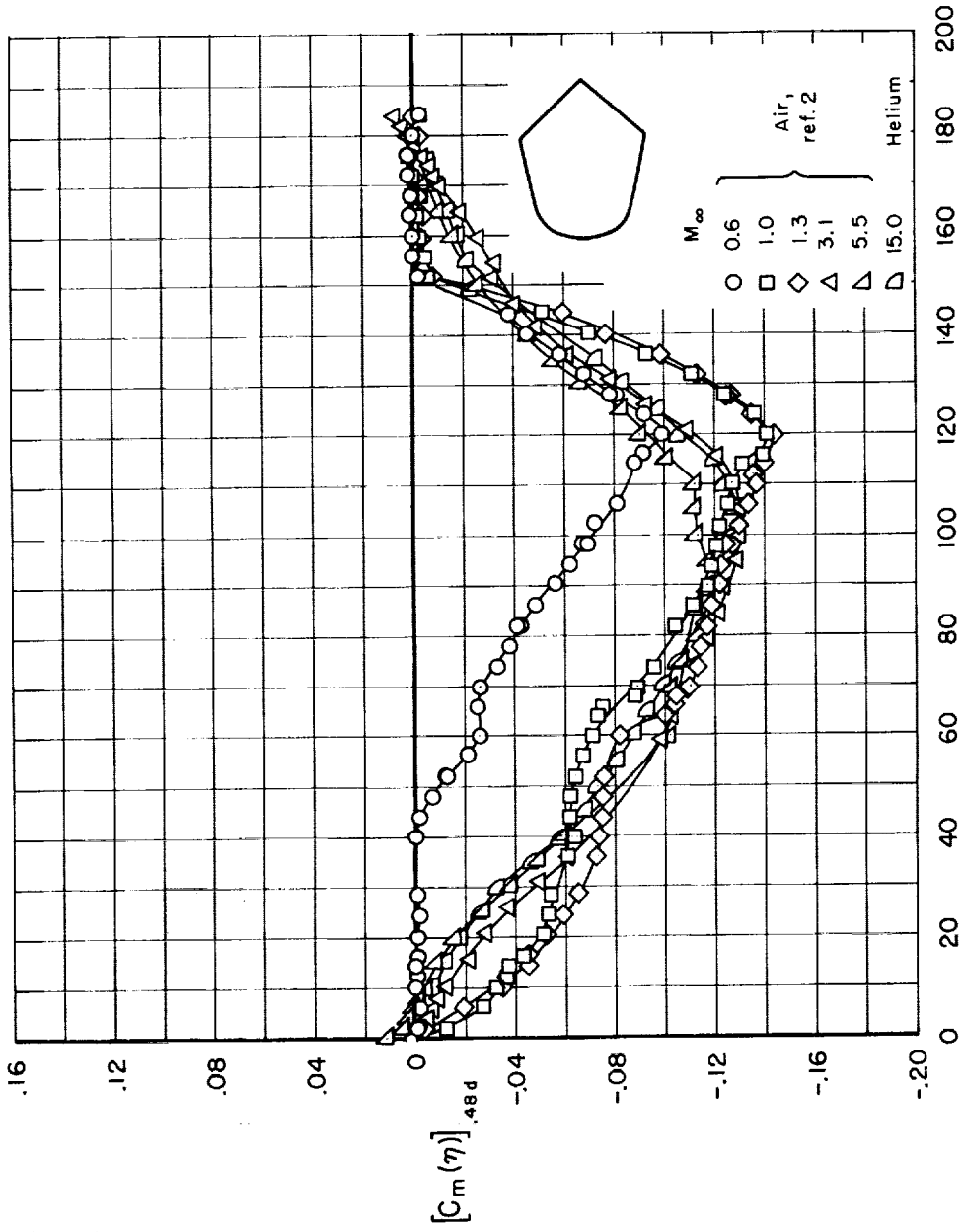

(b) Vehicle with afterbody - Concluded.

Figure 3.- Concluded.

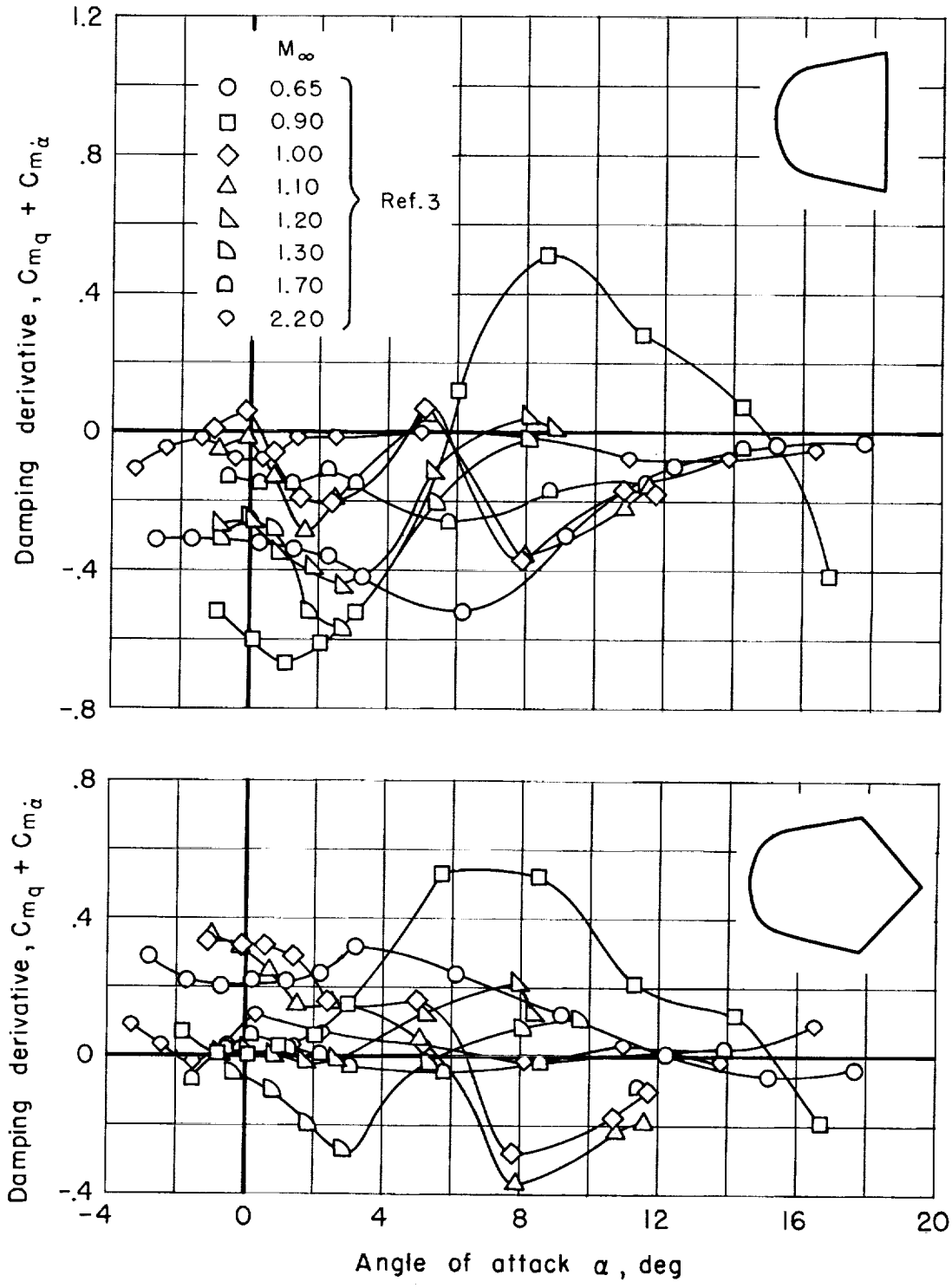

(a) Sting mounted model, forced oscillation data.

Figure 4.- Aerodynamic damping characteristics of vehicles.

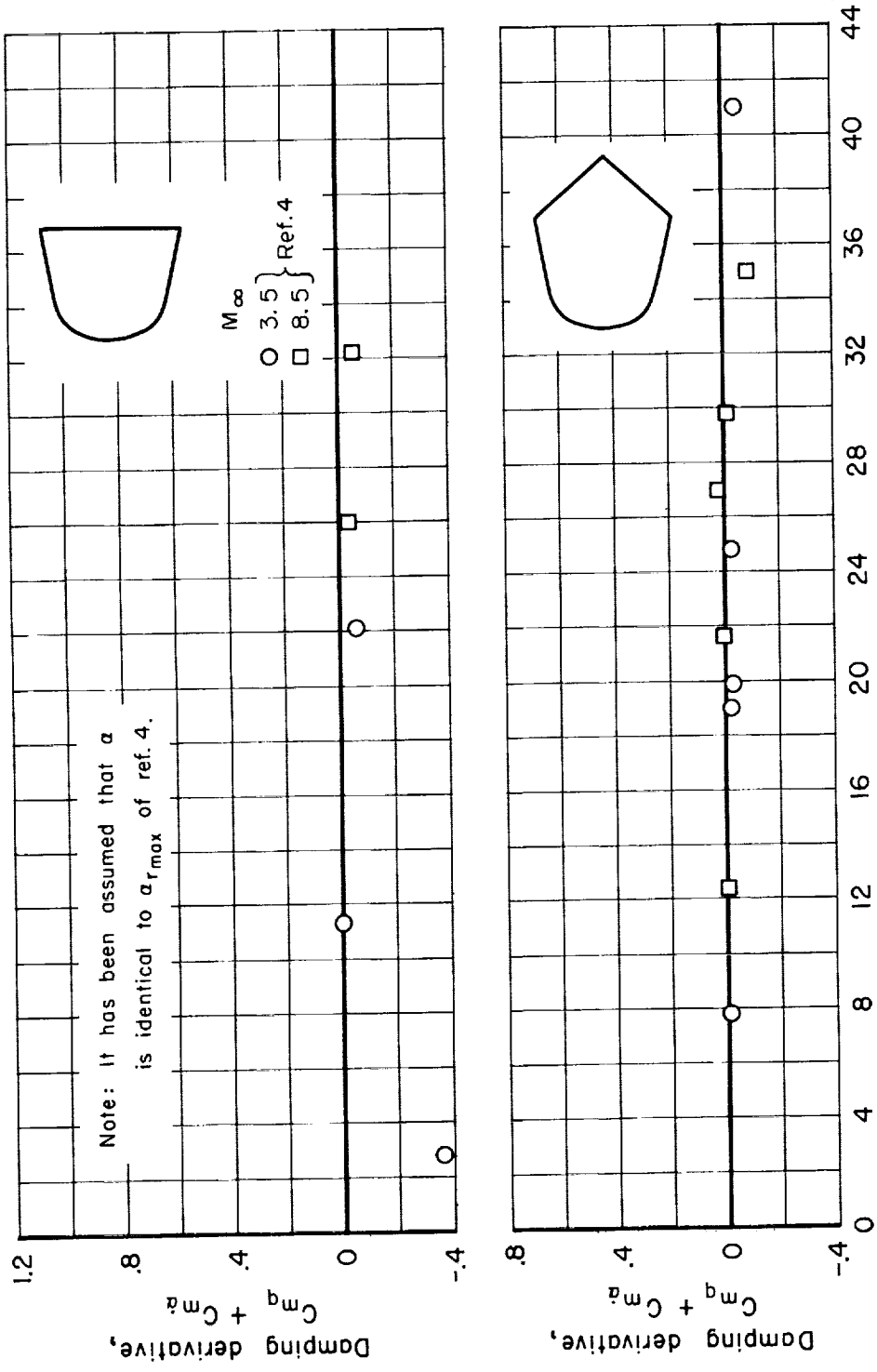

(b) Free-flight data.

Figure 4.- Concluded.

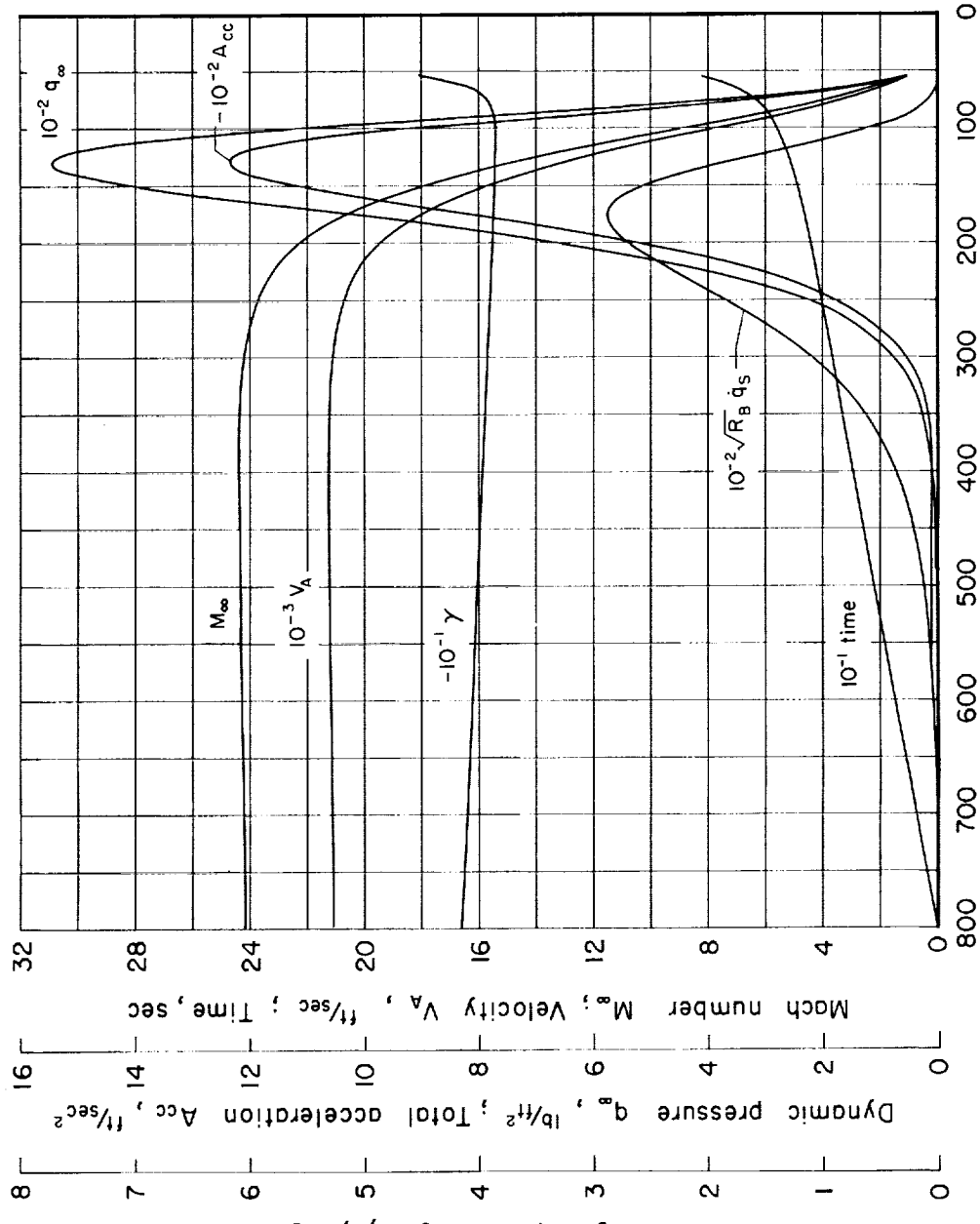

Figure 5.- Trajectory parameters related to motion of vehicle mass center.

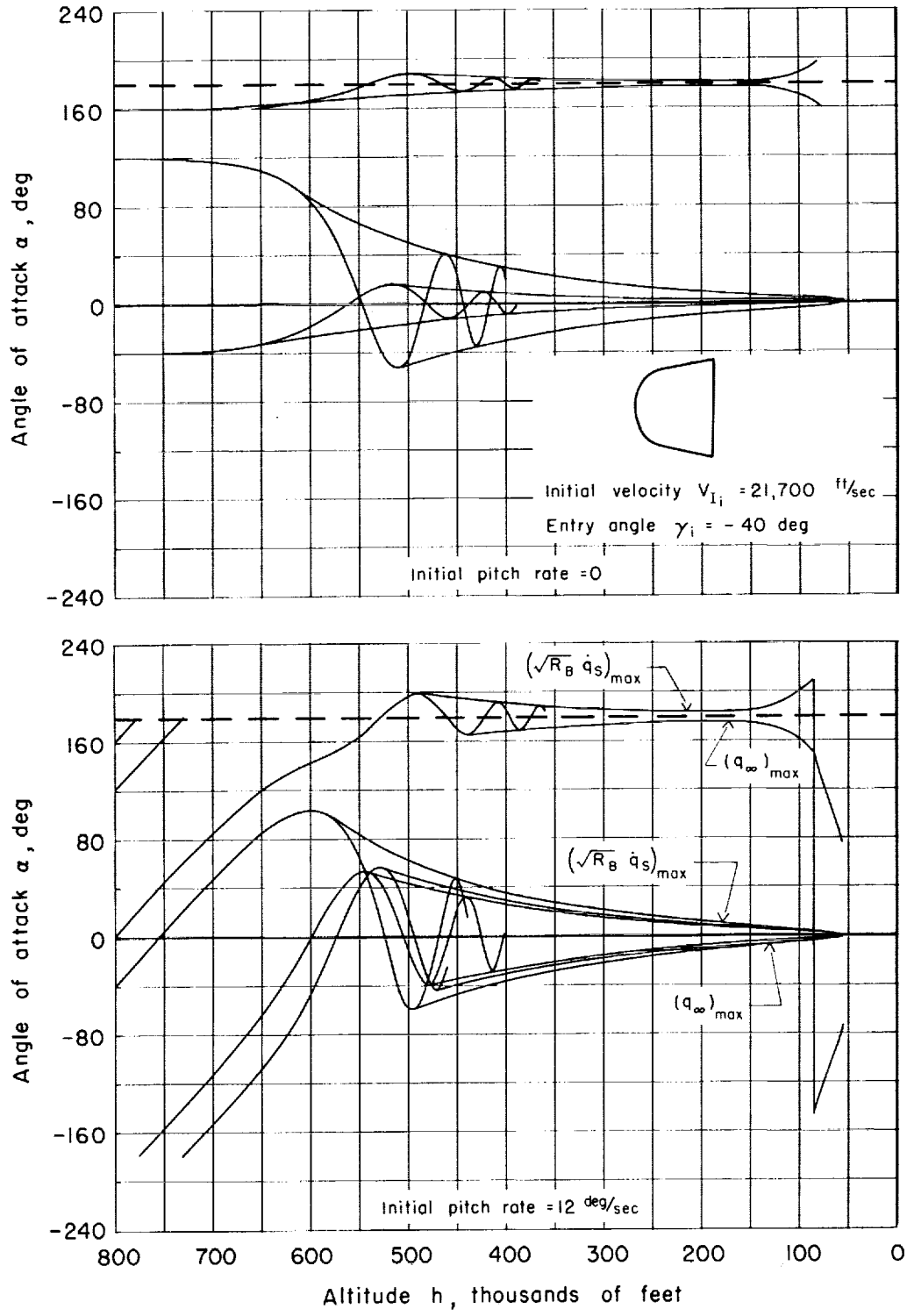

Figure 6.- Altitude history of angle of attack for vehicle statically stable about 0^o and 180^o trim attitudes.

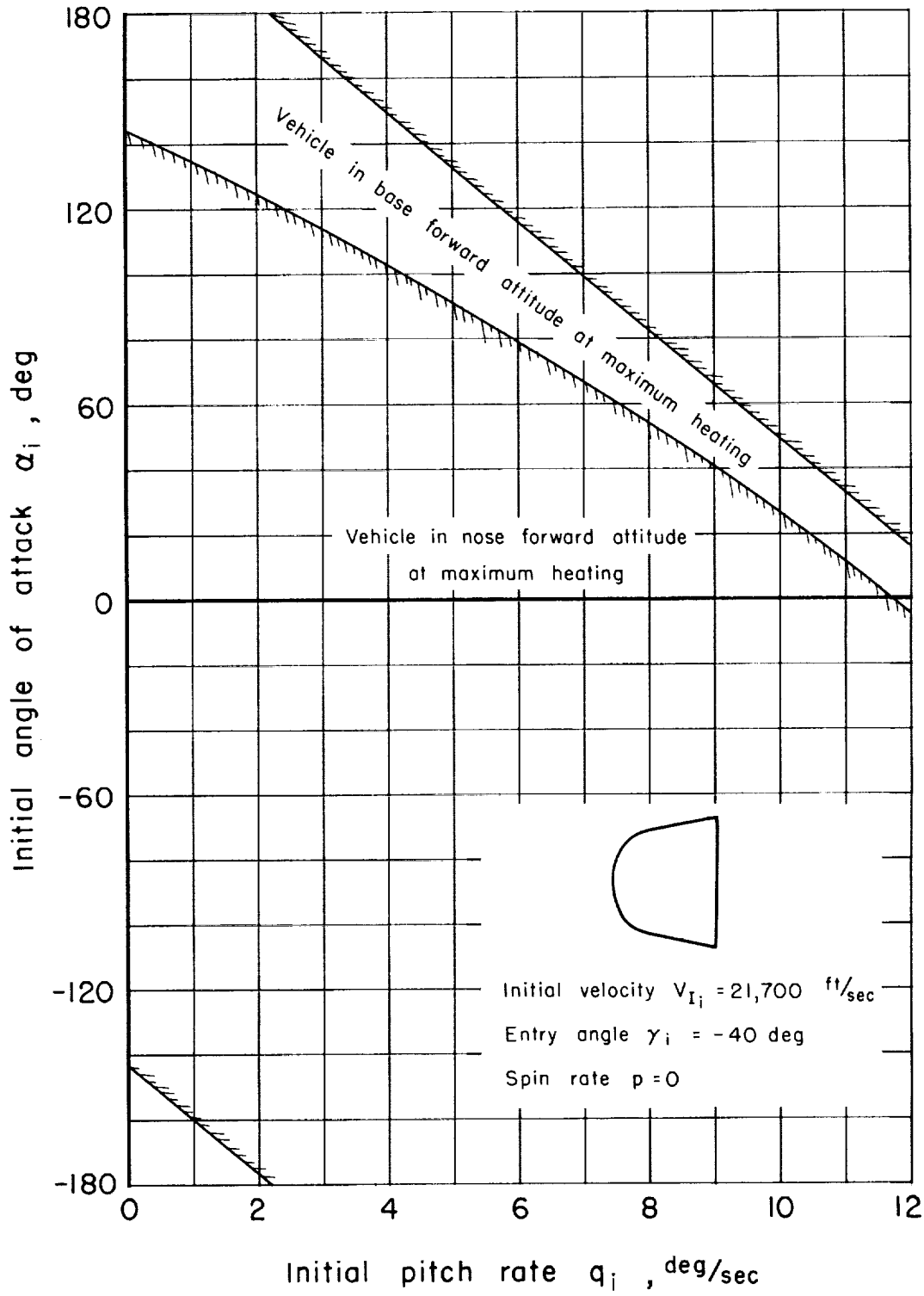

Figure 7.- Relationship between initial conditions and vehicle attitude at maximum heating-rate conditions.

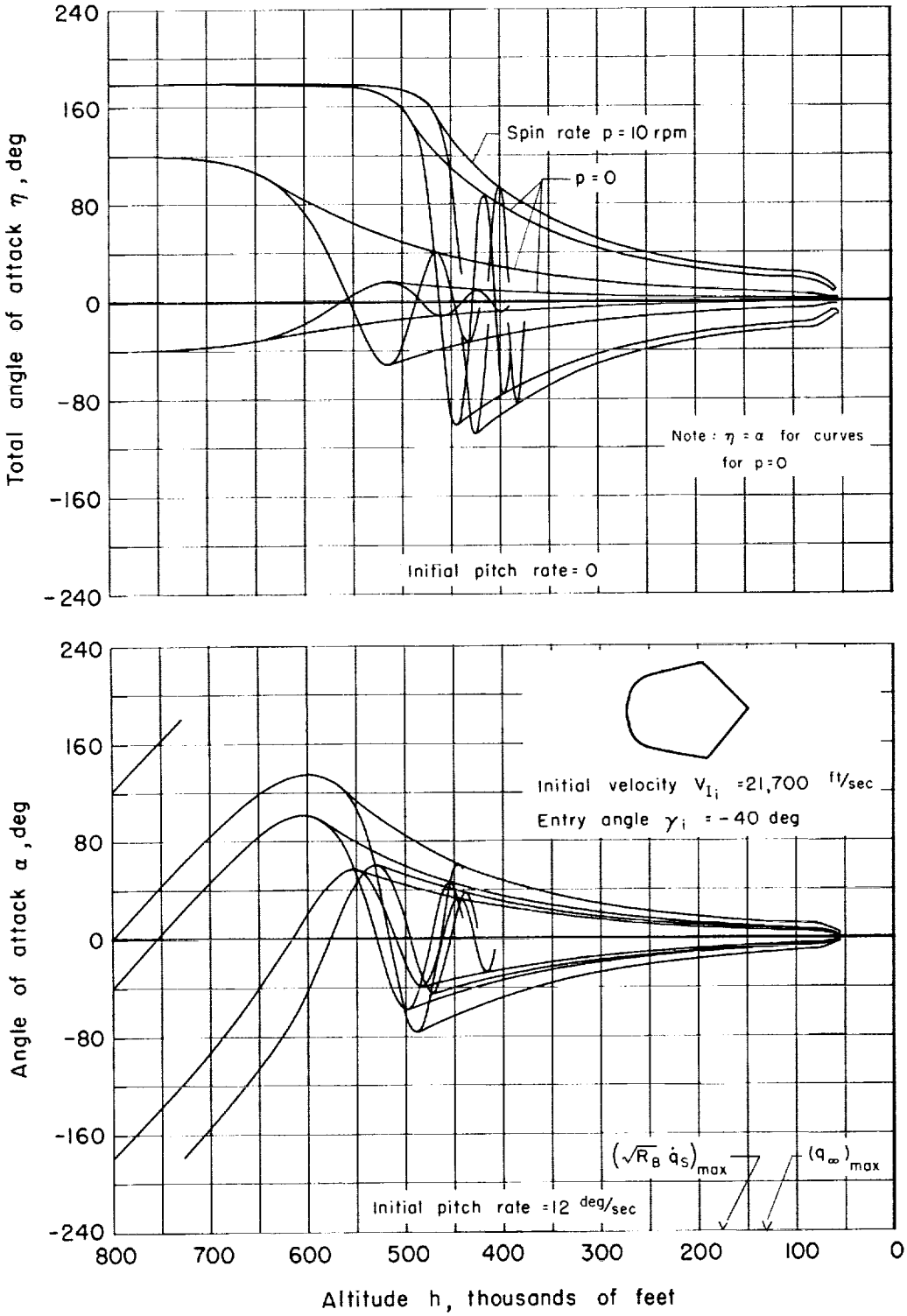

Figure 8.- Attitude history of total angle of attack for vehicle statically stable about 0^o trim attitude.

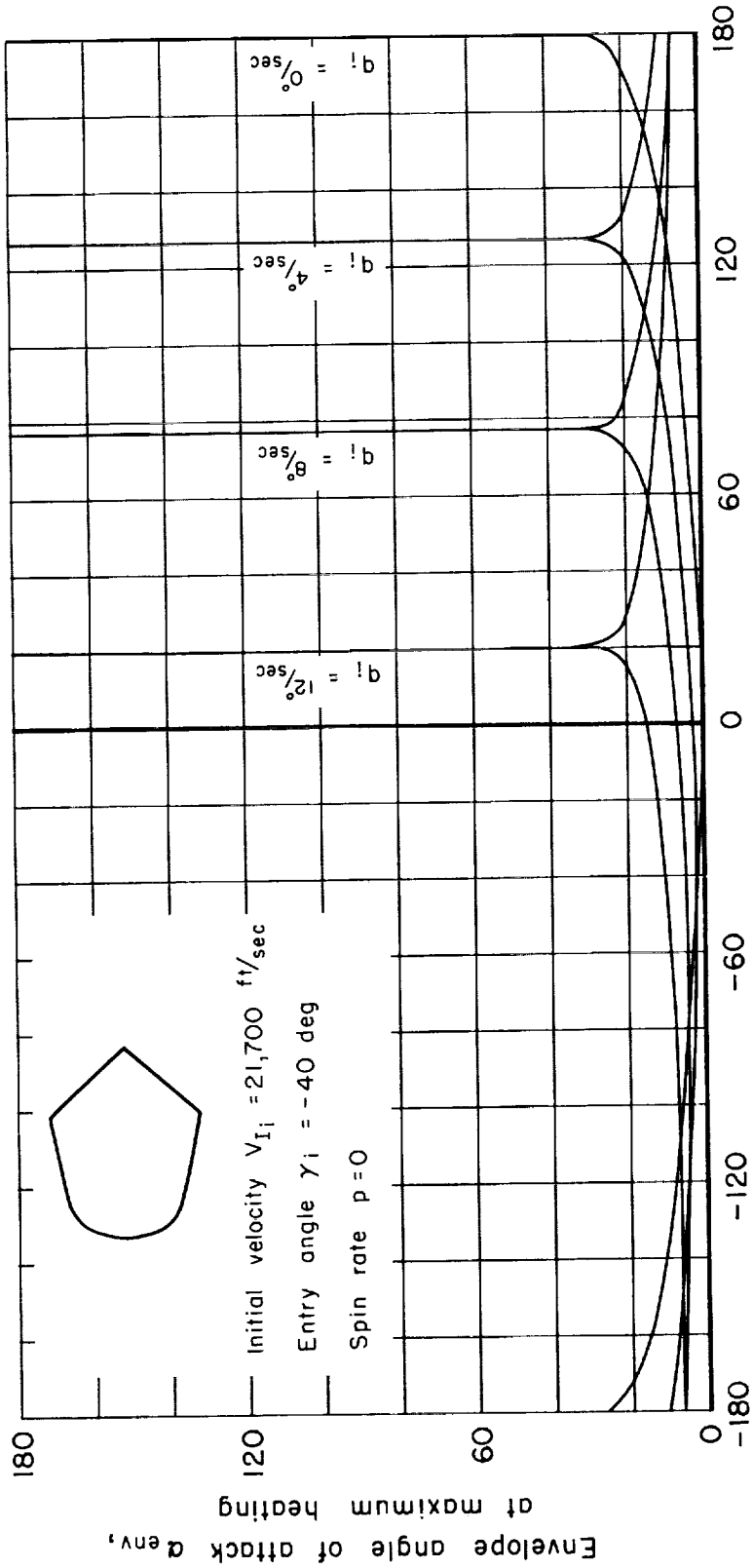

Figure 9.- Relationship between initial conditions and vehicle angle of attack at maximum heating-rate conditions.

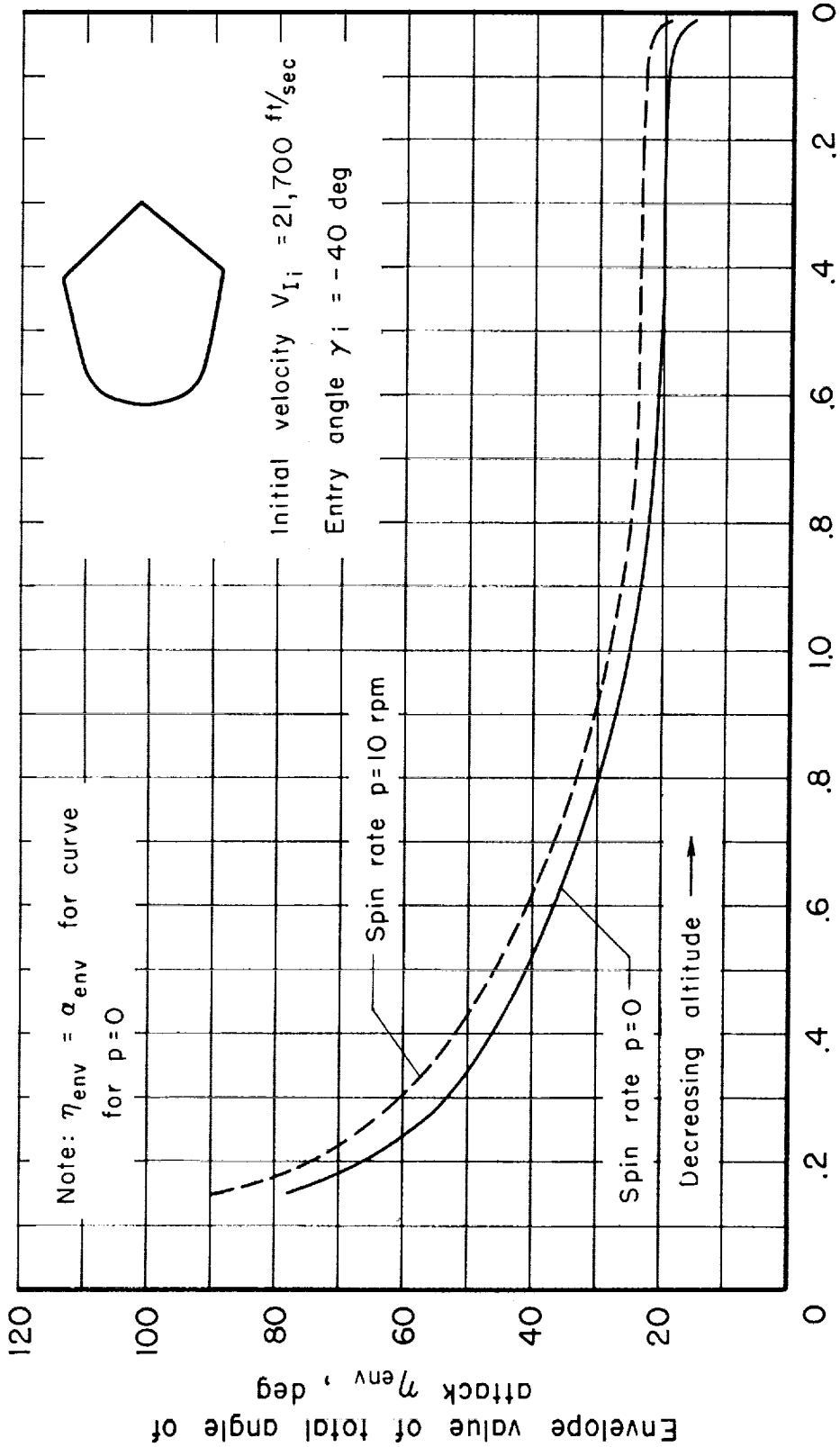

Figure 10.- Relationship between amplitude of oscillatory motion and stagnation point convective heating rate.

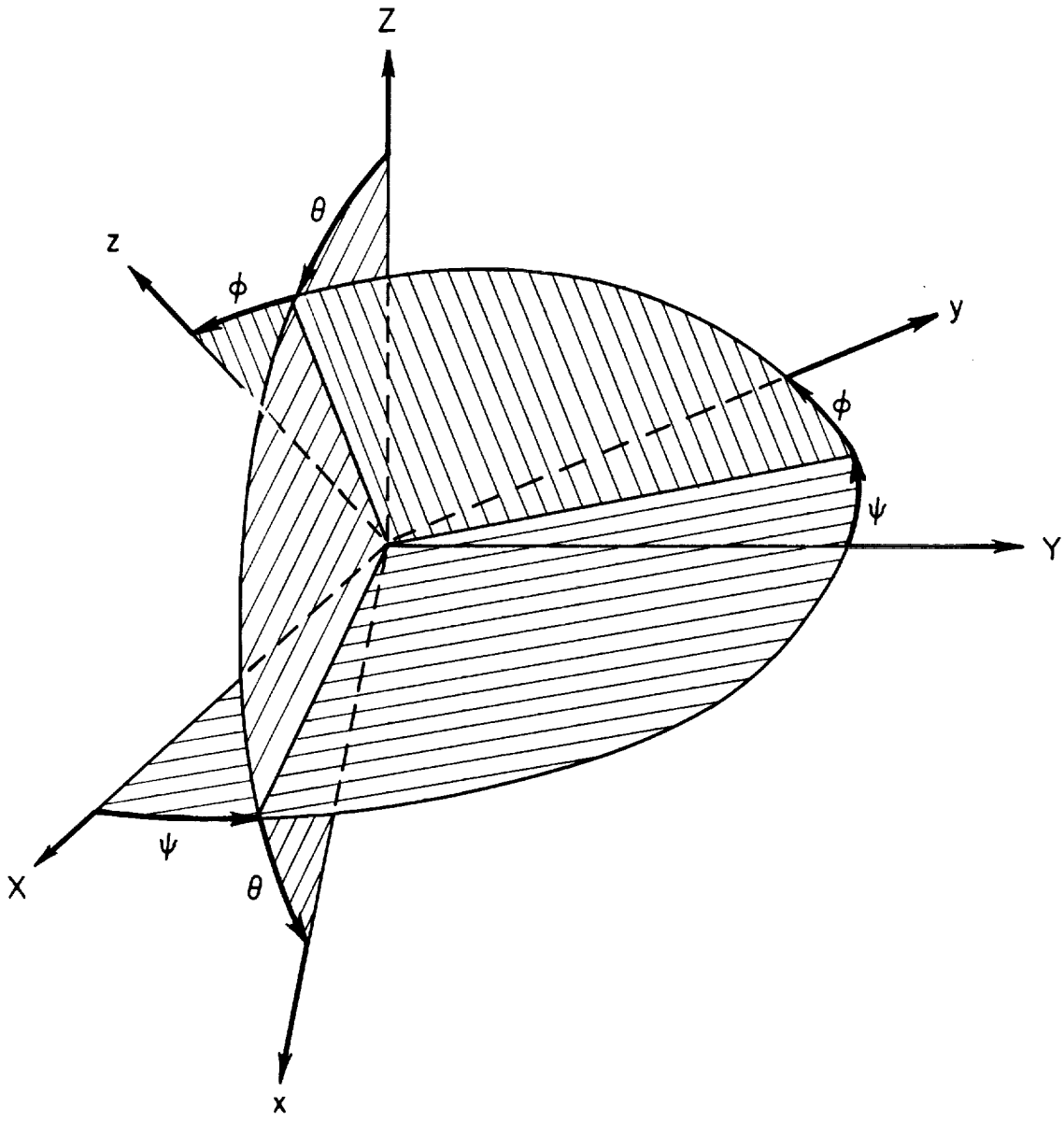

(a) Relationship between inertial axes and body axes.

Figure 11.- Axis systems.

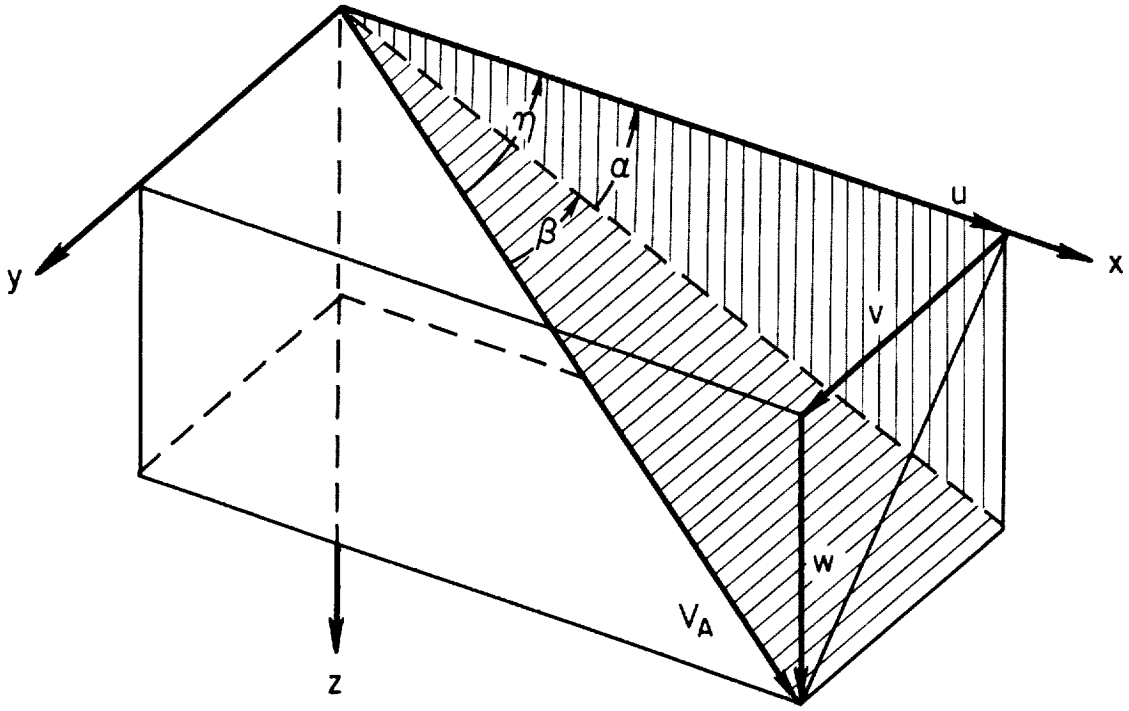

(b) Relationship between aerodynamic velocity and body axes.

Figure 11.- Concluded.

NASA TN D-1326
National Aeronautics and Space Administration.
MOTIONS OF A SHORT 10° BLUNTED CONE ENTERING A MARTIAN ATMOSPHERE AT ARBITRARY ANGLES OF ATTACK AND ARBITRARY PITCHING RATES. Victor L. Peterson. May 1962. 40p. OTS price, $1.00. (NASA TECHNICAL NOTE D-1326)

Dynamic behavior of two vehicles, one with and one without an afterbody, was obtained from machine-calculated solutions of the six-degree-of-freedom rigid-body equations of motion. Experimental static and dynamic aerodynamic characteristics were used in the calculations. The investigation included consideration of a 10-rpm vehicle spin rate and model atmospheres encompassing the probable extremes for the planet.

Copies obtainable from NASA, Washington

I. Peterson, Victor L.
II. NASA TN D-1326

(Initial NASA distribution:
2, Aerodynamics, missiles and space vehicles;
5, Atmospheric entry;
20, Fluid mechanics;
48, Space vehicles;
50, Stability and control.)

NASA

NASA TN D-1326
National Aeronautics and Space Administration.
MOTIONS OF A SHORT 10° BLUNTED CONE ENTERING A MARTIAN ATMOSPHERE AT ARBITRARY ANGLES OF ATTACK AND ARBITRARY PITCHING RATES. Victor L. Peterson. May 1962. 40p. OTS price, $1.00. (NASA TECHNICAL NOTE D-1326)

Dynamic behavior of two vehicles, one with and one without an afterbody, was obtained from machine-calculated solutions of the six-degree-of-freedom rigid-body equations of motion. Experimental static and dynamic aerodynamic characteristics were used in the calculations. The investigation included consideration of a 10-rpm vehicle spin rate and model atmospheres encompassing the probable extremes for the planet.

Copies obtainable from NASA, Washington

I. Peterson, Victor L.
II. NASA TN D-1326

(Initial NASA distribution:
2, Aerodynamics, missiles and space vehicles;
5, Atmospheric entry;
20, Fluid mechanics;
48, Space vehicles;
50, Stability and control.)

NASA

NASA TN D-1326
National Aeronautics and Space Administration.
MOTIONS OF A SHORT 10° BLUNTED CONE ENTERING A MARTIAN ATMOSPHERE AT ARBITRARY ANGLES OF ATTACK AND ARBITRARY PITCHING RATES. Victor L. Peterson. May 1962. 40p. OTS price, $1.00. (NASA TECHNICAL NOTE D-1326)

Dynamic behavior of two vehicles, one with and one without an afterbody, was obtained from machine-calculated solutions of the six-degree-of-freedom rigid-body equations of motion. Experimental static and dynamic aerodynamic characteristics were used in the calculations. The investigation included consideration of a 10-rpm vehicle spin rate and model atmospheres encompassing the probable extremes for the planet.

Copies obtainable from NASA, Washington

I. Peterson, Victor L.
II. NASA TN D-1326

(Initial NASA distribution:
2, Aerodynamics, missiles and space vehicles;
5, Atmospheric entry;
20, Fluid mechanics;
48, Space vehicles;
50, Stability and control.)

NASA

NASA TN D-1326
National Aeronautics and Space Administration.
MOTIONS OF A SHORT 10° BLUNTED CONE ENTERING A MARTIAN ATMOSPHERE AT ARBITRARY ANGLES OF ATTACK AND ARBITRARY PITCHING RATES. Victor L. Peterson. May 1962. 40p. OTS price, $1.00. (NASA TECHNICAL NOTE D-1326)

Dynamic behavior of two vehicles, one with and one without an afterbody, was obtained from machine-calculated solutions of the six-degree-of-freedom rigid-body equations of motion. Experimental static and dynamic aerodynamic characteristics were used in the calculations. The investigation included consideration of a 10-rpm vehicle spin rate and model atmospheres encompassing the probable extremes for the planet.

Copies obtainable from NASA, Washington

I. Peterson, Victor L.
II. NASA TN D-1326

(Initial NASA distribution:
2, Aerodynamics, missiles and space vehicles;
5, Atmospheric entry;
20, Fluid mechanics;
48, Space vehicles;
50, Stability and control.)

NASA

NASA TN D-1326
National Aeronautics and Space Administration.
MOTIONS OF A SHORT 10^{0} BLUNTED CONE ENTERING A MARTIAN ATMOSPHERE AT ARBITRARY ANGLES OF ATTACK AND ARBITRARY PITCHING RATES. Victor L. Peterson. May 1962.
40p. OTS price, $1.00.
(NASA TECHNICAL NOTE D-1326)

Dynamic behavior of two vehicles, one with and one without an afterbody, was obtained from machine-calculated solutions of the six-degree-of-freedom rigid-body equations of motion. Experimental static and dynamic aerodynamic characteristics were used in the calculations. The investigation included consideration of a 10-rpm vehicle spin rate and model atmospheres encompassing the probable extremes for the planet.

Copies obtainable from NASA, Washington

I. Peterson, Victor L.
II. NASA TN D-1326

(Initial NASA distribution:
2, Aerodynamics, missiles and space vehicles;
5, Atmospheric entry;
20, Fluid mechanics;
48, Space vehicles;
50, Stability and control.)

NASA

NASA TN D-1326
National Aeronautics and Space Administration.
MOTIONS OF A SHORT 10^{0} BLUNTED CONE ENTERING A MARTIAN ATMOSPHERE AT ARBITRARY ANGLES OF ATTACK AND ARBITRARY PITCHING RATES. Victor L. Peterson. May 1962.
40p. OTS price, $1.00.
(NASA TECHNICAL NOTE D-1326)

Dynamic behavior of two vehicles, one with and one without an afterbody, was obtained from machine-calculated solutions of the six-degree-of-freedom rigid-body equations of motion. Experimental static and dynamic aerodynamic characteristics were used in the calculations. The investigation included consideration of a 10-rpm vehicle spin rate and model atmospheres encompassing the probable extremes for the planet.

Copies obtainable from NASA, Washington

I. Peterson, Victor L.
II. NASA TN D-1326

(Initial NASA distribution:
2, Aerodynamics, missiles and space vehicles;
5, Atmospheric entry;
20, Fluid mechanics;
48, Space vehicles;
50, Stability and control.)

NASA

NASA TN D-1326
National Aeronautics and Space Administration.
MOTIONS OF A SHORT 10^{0} BLUNTED CONE ENTERING A MARTIAN ATMOSPHERE AT ARBITRARY ANGLES OF ATTACK AND ARBITRARY PITCHING RATES. Victor L. Peterson. May 1962.
40p. OTS price, $1.00.
(NASA TECHNICAL NOTE D-1326)

Dynamic behavior of two vehicles, one with and one without an afterbody, was obtained from machine-calculated solutions of the six-degree-of-freedom rigid-body equations of motion. Experimental static and dynamic aerodynamic characteristics were used in the calculations. The investigation included consideration of a 10-rpm vehicle spin rate and model atmospheres encompassing the probable extremes for the planet.

Copies obtainable from NASA, Washington

I. Peterson, Victor L.
II. NASA TN D-1326

(Initial NASA distribution:
2, Aerodynamics, missiles and space vehicles;
5, Atmospheric entry;
20, Fluid mechanics;
48, Space vehicles;
50, Stability and control.)

NASA

NASA TN D-1326
National Aeronautics and Space Administration.
MOTIONS OF A SHORT 10^{0} BLUNTED CONE ENTERING A MARTIAN ATMOSPHERE AT ARBITRARY ANGLES OF ATTACK AND ARBITRARY PITCHING RATES. Victor L. Peterson. May 1962.
40p. OTS price, $1.00.
(NASA TECHNICAL NOTE D-1326)

Dynamic behavior of two vehicles, one with and one without an afterbody, was obtained from machine-calculated solutions of the six-degree-of-freedom rigid-body equations of motion. Experimental static and dynamic aerodynamic characteristics were used in the calculations. The investigation included consideration of a 10-rpm vehicle spin rate and model atmospheres encompassing the probable extremes for the planet.

Copies obtainable from NASA, Washington

I. Peterson, Victor L.
II. NASA TN D-1326

(Initial NASA distribution:
2, Aerodynamics, missiles and space vehicles;
5, Atmospheric entry;
20, Fluid mechanics;
48, Space vehicles;
50, Stability and control.)

NASA